

# Nonlinear spin-motive force driven by mixed-space quantum geometry

Tomonari Meguro<sup>1,\*</sup>, Hiroaki Ishizuka<sup>2,†</sup> and Kentaro Nomura<sup>1,3‡</sup>

<sup>1</sup>*Department of Physics, Kyushu University, Fukuoka 819-0395, Japan*

<sup>2</sup>*Department of Physics, Institute of Science Tokyo, Meguro, Tokyo 152-8551, Japan*

<sup>3</sup>*Quantum and Spacetime Research Institute, Kyushu University, Fukuoka, 819-0395, Japan*

(Dated: March 13, 2026)

Spin-motive force, i.e., the electric current induced by magnetization dynamics, is theoretically studied beyond the Thouless-pump paradigm. In contrast to the linear-response regime, where the induced current is purely AC, we show that spin-motive force acquires both a DC component and a second-harmonic component at nonlinear order in magnetization dynamics. We further clarify that both contributions originate from the geometric properties of electronic bands — quantum geometry defined in the mixed parameter space  $(\mathbf{k}, \mathbf{m})$  spanned by electron’s momentum  $\mathbf{k}$  and magnetization  $\mathbf{m}$ . By applying the theory to a Luttinger model, we demonstrate that our mechanism yields a finite nonlinear current even in the insulating regime, and the resulting electrical signal is measurable in a conventional current-measurement setup. Our findings offer a new operating principle of AC-to-DC conversion with magnetic materials, highlighting the pivotal role of the  $(\mathbf{k}, \mathbf{m})$ -mixed space quantum geometry in magnetization-dynamics-induced electric currents.

## I. INTRODUCTION

The efficient and flexible interconversion between spin and charge degrees of freedom is one of the central aims of spintronics [1–3]. Spin-to-charge conversion, in particular, provides an electrical route to probe and utilize the magnetization dynamics in magnetic materials and junction systems. A paradigmatic example is the spin-motive force (SMF), in which time-dependent magnetization can generate an electromotive force and drive an electric current. Originally, the SMF was discussed for spatially inhomogeneous magnetic textures, such as domain walls and skyrmions [4–13], and has since been experimentally observed in a wide range of materials [7, 14–18]. Later on, it has also been shown that a spatial gradient of magnetization is not a prerequisite; in the presence of spin-orbit interaction, a uniform magnetization undergoing temporal variation can induce an electric current [19–22]; they are also referred to as the SMF in a narrower sense. Despite extensive studies of SMF in various systems, the discussion has been largely limited to the linear-response regime, where the resulting electric current is proportional to the time derivative of magnetization. Beyond linear response, one may expect spin-to-charge conversion to enable rectification and higher-harmonic generation. Such nonlinear effects provide key functionalities for flexible electrical readout and frequency conversion driven by magnetization dynamics—an aspect that has remained largely unexplored.

In the study of nonlinear responses, it has been increasingly recognized that the geometrical properties of electronic states, collectively termed quantum geometry, play crucial roles [23–27]. Key quantities that characterize the geometry of quantum states are the metric and

curvature in the parameter space on which the quantum states are defined, known as the quantum metric and the Berry curvature, respectively. Historically, the importance of the Berry curvature has long been recognized in the context of linear electrical transport [23, 24], such as in the quantum and anomalous Hall effects; they are related to the Berry curvature of Bloch states in the crystal momentum  $(\mathbf{k})$  space. Recently, the role of the quantum metric in nonlinear responses has also been actively discussed [25–27]. Studies of the nonlinear Hall effect [28–30] have revealed that the response coefficients can be expressed in terms of the quantum metric or the Berry curvature-dipole. These findings have offered not only a new way of understanding electrical responses, but also design principles for functional materials and electronic devices with rectifying and high-frequency sensing capabilities [31–33]. To date, the role of  $\mathbf{k}$ -space quantum geometry in material responses has been well established, both theoretically and experimentally.

These developments motivate revisiting spin-charge conversion from a quantum geometric viewpoint. Extending this viewpoint to spintronics naturally leads to the quantum geometry of the  $(\mathbf{k}, \mathbf{m})$ -mixed space, in which the magnetization  $\mathbf{m}$  is considered an additional parameter. Indeed, the observation of intrinsic spin-orbit torque [34] and a subsequent theoretical analysis [35] opened a pathway toward understanding charge-spin conversions as a phenomenon related to the  $(\mathbf{k}, \mathbf{m})$ -mixed space quantum geometry [22, 36–45]. For SMF, theoretical studies have proposed that the effect originates from the Berry curvature defined in the  $(\mathbf{k}, \mathbf{m})$ -mixed space [22, 41, 42]. However, most existing studies have focused on the linear-response regime,  $\mathbf{j} \approx J_{\text{ex}} \dot{\mathbf{m}}$ , where  $J_{\text{ex}}$  is the exchange coupling constant between the electron spin and the magnetization. In that regime, the induced electric current remains purely AC, without a DC component or frequency-converted components; it oscillates in time, and the average current over a cycle of magnetization precession vanishes. Furthermore, pre-

\* meguro.tomonari@mbp.phys.kyushu-u.ac.jp

† ishizuka@hiroishizuka.com

‡ nomura.kentaro@mbp.phys.kyushu-u.ac.jp

ceding theoretical works have concentrated on the Berry curvature contribution, leaving the role of the quantum metric unclarified. A theory of nonlinear SMF based on mixed-space quantum geometry is needed to clarify how magnetization dynamics generates finite cycle-averaged and higher-harmonic responses, and how these signals are linked to the geometric properties of electronic states.

In this work, we develop a theory of SMF in the nonlinear regime from the perspective of quantum geometry in the  $(\mathbf{k}, \mathbf{m})$ -mixed space. Considering a ferromagnet in which the spatially homogeneous magnetization varies in time, we formulate the electric current response to second order in the magnetization dynamics, using semiclassical wave-packet theory. Consequently, we find that a nonlinear SMF exhibits DC and second harmonic generation (SHG) under precessional magnetization dynamics. We further demonstrate that their geometric origins are distinguished by frequency scaling; contributions linear in the precession frequency are governed by the Berry curvature, whereas those quadratic in frequency are governed by the quantum metric, both of which are defined in the  $(\mathbf{k}, \mathbf{m})$ -mixed space. To illustrate the significance of the nonlinear SMF, we perform numerical calculations in a Luttinger model. As a result, we find that, even in the insulating regime, our mechanism yields a finite nonlinear SMF, and the resulting signal is detectable in a standard current measurement. Our findings suggest that quantum geometry in the mixed space plays a pivotal role in the field of nonlinear spintronics.

## II. WAVE-PACKET THEORY

### A. Wave-packet

To study the effect of magnetization dynamics on electron dynamics, we consider a Hamiltonian that consists of a static term and time-dependent terms which are treated perturbatively. The Hamiltonian reads,

$$\hat{H}(t) = \hat{H}^{(0)} + \sum_{\beta} \delta m_{\beta}(t) \hat{H}'_{\beta}. \quad (1)$$

where  $\beta = x, y, z$ . We assume the static term  $\hat{H}^{(0)}$  consists of temporally uniform terms, such as the electron kinetic energy, the crystal potential, and the static magnetization  $\mathbf{m}_0$ , and potentials that vary slowly compared to the lattice spacing, such as the electromagnetic potential by external fields. In the time-dependent parts,  $\delta m_{\beta}(t)$  is assumed to be small,  $\delta m \ll m_0$  ( $\delta m = |\delta \mathbf{m}(t)|$  and  $m_0 = |\mathbf{m}_0|$ ). In addition,  $\delta m_{\beta}(t)$  is periodic in time with  $T$  and changes slowly such that  $\hbar/T$  is sufficiently small compared to the energy scale of  $\hat{H}^{(0)}$ .

Following the semiclassical theory for electron dynamics [28, 46], we consider the dynamics of a wave-packet-type wavefunction localized at  $\mathbf{x}_c, \mathbf{k}_c$  in the Liouville space. Here,  $\mathbf{x}_c$  and  $\mathbf{k}_c$  are the center of mass of the

wave packet in the real and momentum space, respectively. The time-evolution of the wave packet is determined by a variational method. To this end, we consider a situation such that the slowly-varying potential in  $\hat{H}^{(0)}$  is the electrostatic potential  $\phi(\mathbf{x})$  [47]. Defining the Bloch Hamiltonian for  $\hat{H}^{(0)}$  as  $\hat{\mathcal{H}}_{\mathbf{k}}^{(0)} = e^{i\mathbf{k}\cdot\hat{\mathbf{x}}} \hat{H}^{(0)} e^{-i\mathbf{k}\cdot\hat{\mathbf{x}}}$ , one can obtain the Bloch eigenstates and values as

$$\hat{\mathcal{H}}_{\mathbf{k}}^{(0)} |u_{n\mathbf{k}}^{(0)}(\mathbf{m}_0)\rangle = \varepsilon_{n\mathbf{k}}^{(0)}(\mathbf{x}_c, \mathbf{m}_0) |u_{n\mathbf{k}}^{(0)}(\mathbf{m}_0)\rangle, \quad (2)$$

where  $\mathbf{k}$  is the crystal momentum. The electrostatic potential merely shifts the eigenvalues, and the Bloch eigenstates do not depend on  $\mathbf{x}_c$ . Using this local Bloch eigenstates, we construct the wave-packet by

$$|\Psi_{\mathbf{x}_c, \mathbf{k}_c}\rangle = \int_{\mathbf{k}} e^{i\mathbf{k}\cdot\hat{\mathbf{x}}} \left[ \sum_l C_{l\mathbf{k}}(\mathbf{x}_c, \mathbf{k}_c, t) |u_{l\mathbf{k}}^{(0)}(\mathbf{m}_0)\rangle \right], \quad (3)$$

where  $\int_{\mathbf{k}} \equiv \int_{\text{BZ}} d^d \mathbf{k} / (2\pi)^d$  denotes the momentum integral in the Brillouin zone (BZ). The coefficients  $C_{l\mathbf{k}}(\mathbf{x}_c, \mathbf{k}_c, t)$  are chosen such that the wave function is sharply peaked at  $\mathbf{x}_c$  in the real space and at  $\mathbf{k}_c$  in the momentum space, i.e.,  $\mathbf{x}_c = \langle \overline{\Psi_{\mathbf{x}_c, \mathbf{k}_c}} | \hat{\mathbf{x}} | \overline{\Psi_{\mathbf{x}_c, \mathbf{k}_c}} \rangle$  and  $\mathbf{k}_c = \langle \overline{\Psi_{\mathbf{x}_c, \mathbf{k}_c}} | \hat{\mathbf{k}} | \overline{\Psi_{\mathbf{x}_c, \mathbf{k}_c}} \rangle$ , where

$$|\overline{\Psi_{\mathbf{x}_c, \mathbf{k}_c}}\rangle = \frac{|\Psi_{\mathbf{x}_c, \mathbf{k}_c}\rangle}{\sqrt{\langle \overline{\Psi_{\mathbf{x}_c, \mathbf{k}_c}} | \Psi_{\mathbf{x}_c, \mathbf{k}_c} \rangle}} \quad (4)$$

is the normalized wave-packet. In most cases, the wave-packet is assumed to be confined in a band, which we denote as the  $n$ -th band, i.e.,  $C_{l\mathbf{k}}(\mathbf{x}_c, \mathbf{k}_c, t) = 0$  ( $l \neq n$ ). In this work, however, we consider the effect of inter-band transition, which we assume to be  $|C_{l\mathbf{k}}(\mathbf{x}_c, \mathbf{k}_c, t)| \ll |C_{n\mathbf{k}}(\mathbf{x}_c, \mathbf{k}_c, t)|$  ( $l \neq n$ ).

In principle, one may choose any form for the coefficient  $C_{l\mathbf{k}}(\mathbf{x}_c, \mathbf{k}_c, t)$  for  $l \neq n$  in Eq. (3). In the current case, as a natural choice of  $C_{l\mathbf{k}}(\mathbf{x}_c, \mathbf{k}_c, t)$ , we choose the coefficient based on the first order perturbation theory. Therefore, we require that the wave-packet given in Eq. (3) follows the time-dependent Schrödinger equation,

$$i\hbar \partial_t |\Psi_{\mathbf{x}_c, \mathbf{k}_c}\rangle = \left( \hat{H}^{(0)} + \sum_{\beta} \delta m_{\beta}(t) \hat{H}'_{\beta} \right) |\Psi_{\mathbf{x}_c, \mathbf{k}_c}\rangle. \quad (5)$$

Here, the time dependence of the wave-packet comes from both  $C_{l\mathbf{k}}(\mathbf{x}_c, \mathbf{k}_c, t)$  explicitly and centers of mass implicitly. Assuming that  $\sum_{\beta} \delta m_{\beta}(t) \hat{H}'_{\beta}$  is a small correction to  $\hat{H}^{(0)}$ , we find that the coefficient reads (see Appendix A for the derivation),

$$C_{l\mathbf{k}}(\mathbf{x}_c, \mathbf{k}_c, t) = M_{l\mathbf{k}}(\mathbf{x}_c, \mathbf{k}_c, t) C_{n\mathbf{k}}(\mathbf{x}_c, \mathbf{k}_c, t), \quad (6)$$

$$M_{l\mathbf{k}}^{(1)}(\mathbf{x}_c, \mathbf{k}_c, t) = - \sum_{\beta, \Omega} \frac{\delta m_{\Omega, \beta} e^{-i\Omega t}}{\varepsilon_{l\mathbf{k}}^{(0)}(\mathbf{x}_c, \mathbf{m}_0) - \hbar\Omega} (\hat{H}'_{\beta})_{l\mathbf{k}} \quad (7)$$

where  $\delta m_{\beta}(t)$  is expanded with its discrete Fourier components,  $\delta m_{\beta}(t) = \sum_{\Omega} \delta m_{\Omega, \beta} e^{-i\Omega t}$ . We assume that  $C_{l\mathbf{k}}(\mathbf{x}_c, \mathbf{k}_c, t)$  differs from  $C_{n\mathbf{k}}(\mathbf{x}_c, \mathbf{k}_c, t)$  only by an

overall factor  $M_{ln,\mathbf{k}}(\mathbf{x}_c, \mathbf{k}_c, t)$ ; this assumption is supported by the perturbation theory, in which  $M^{(1)}$  gives the first order correction. We further expand  $M_{ln}$  in power of  $\delta m$ ,  $M_{ln}(\mathbf{x}_c, \mathbf{k}_c, t) = \sum_{N \geq 1} M_{ln}^{(N)}(\mathbf{x}_c, \mathbf{k}_c, t)$ , where  $M_{ln}^{(N)}(\mathbf{x}_c, \mathbf{k}_c, t)$  is  $\mathcal{O}(\delta m^N)$ . In the denominator,  $\varepsilon_{ln,\mathbf{k}}^{(0)}(\mathbf{x}_c, \mathbf{m}_0) = \varepsilon_{l\mathbf{k}}^{(0)}(\mathbf{x}_c, \mathbf{m}_0) - \varepsilon_{n\mathbf{k}}^{(0)}(\mathbf{x}_c, \mathbf{m}_0)$  denotes the difference of energy between the eigenstates in  $l$ -th and  $n$ -th bands, and  $(\hat{H}'_\beta)_{ln} = \langle u_{l\mathbf{k}}^{(0)}(\mathbf{m}_0) | \hat{H}'_\beta | u_{n\mathbf{k}}^{(0)}(\mathbf{m}_0) \rangle$  is a matrix element for the perturbative Hamiltonian that is expressed by the unperturbed Bloch eigenstates.

Consequently, the wave-packet wavefunction in Eq. (3) reads

$$|\Psi_{\mathbf{x}_c, \mathbf{k}_c}\rangle = \int_{\mathbf{k}} e^{i\mathbf{k} \cdot \hat{\mathbf{x}}} C_n(\mathbf{x}_c, \mathbf{k}_c, t) |\tilde{u}_{n\mathbf{k}}(\mathbf{x}_c, \mathbf{m})\rangle, \quad (8)$$

where  $|\tilde{u}_{n\mathbf{k}}(\mathbf{x}_c, \mathbf{m})\rangle$  are the Bloch eigenstates of the Hamiltonian  $\hat{H}(t) = \hat{H}^{(0)} + \sum_\beta \delta m_\beta(t) \hat{H}'_\beta$  up to the first order in  $\delta m_\beta$ , and are given by  $|\tilde{u}_{n\mathbf{k}}(\mathbf{x}_c, \mathbf{m})\rangle = |u_{n\mathbf{k}}^{(0)}(\mathbf{m}_0)\rangle + |u_{n\mathbf{k}}^{(1)}(\mathbf{x}_c, \mathbf{m})\rangle + \dots$  with

$$|u_{n\mathbf{k}}^{(1)}(\mathbf{x}_c, \mathbf{m})\rangle = \sum_{l(\neq n)} M_{ln}^{(1)}(\mathbf{x}_c, \mathbf{k}_c, t) |u_{l\mathbf{k}}^{(0)}(\mathbf{m}_0)\rangle. \quad (9)$$

Using these results, the normalized wavefunction up to the second order in  $\delta m$  reads,

$$\begin{aligned} |\overline{\Psi_{\mathbf{x}_c, \mathbf{k}_c}}\rangle &= \frac{|\Psi_{\mathbf{x}_c, \mathbf{k}_c}\rangle}{\sqrt{1 + \langle \Psi_{\mathbf{x}_c, \mathbf{k}_c}^{(1)} | \Psi_{\mathbf{x}_c, \mathbf{k}_c}^{(1)} \rangle + \mathcal{O}(\delta m^3)}} \\ &= (1 + \delta) |\Psi_{\mathbf{x}_c, \mathbf{k}_c}^{(0)}\rangle + |\Psi_{\mathbf{x}_c, \mathbf{k}_c}^{(1)}\rangle + |\Psi_{\mathbf{x}_c, \mathbf{k}_c}^{(2)}\rangle + \dots, \end{aligned} \quad (10)$$

where  $|\Psi_{\mathbf{x}_c, \mathbf{k}_c}^{(N)}\rangle \propto \mathcal{O}(\delta m^N)$  and  $\delta = -\frac{1}{2} \langle \Psi_{\mathbf{x}_c, \mathbf{k}_c}^{(1)} | \Psi_{\mathbf{x}_c, \mathbf{k}_c}^{(1)} \rangle$ .

### B. Equations of motion

The dynamics of the wave-packet is determined by the extrema of action, which reads

$$S = \int dt L[\mathbf{x}_c(t), \mathbf{k}_c(t)], \quad (11)$$

where  $L[\mathbf{x}_c(t), \mathbf{k}_c(t)]$  is the Lagrangian. Using the normalized wavefunction, the Lagrangian for Eq. (10) reads (the detailed derivation is presented in Appendix.B)

$$\begin{aligned} L &= \langle \overline{\Psi_{\mathbf{x}_c, \mathbf{k}_c}} | \left( i\hbar \frac{d}{dt} - \hat{H}(t) \right) | \overline{\Psi_{\mathbf{x}_c, \mathbf{k}_c}} \rangle \\ &= \hbar \dot{\mathbf{x}}_c \cdot \mathbf{k}_c - \tilde{\mathcal{E}}_n - \phi(\mathbf{x}_c) \\ &\quad - \hbar \dot{\mathbf{k}}_c \cdot \tilde{\mathbf{A}}_n^{\mathbf{k}_c} - \hbar \dot{\mathbf{m}} \cdot \tilde{\mathbf{A}}_n^{\mathbf{m}}, \end{aligned} \quad (12)$$

where  $\tilde{\mathbf{A}}_n^{\mathbf{k}_c} = -i \langle \tilde{u}_{n\mathbf{k}_c}(\mathbf{x}_c, \mathbf{m}) | \partial_{\mathbf{k}_c} | \tilde{u}_{n\mathbf{k}_c}(\mathbf{x}_c, \mathbf{m}) \rangle$  is the Berry connection with the perturbative correction, and  $\tilde{\mathbf{A}}_n^{\mathbf{m}}$  is defined in the same manner but with the derivatives with respect to  $\mathbf{m}$ . We ignore the Berry connection

with respect to  $\mathbf{x}_c$  under the approximation that neglects terms of second or higher order in the product of  $\delta m$  and the spatial gradient, since it is not the main focus of this study. The energy of the  $n$ -th wave-packet consists of two terms,  $\tilde{\mathcal{E}}_n = \tilde{\mathcal{E}}_n^{\text{WP}} + \tilde{\mathcal{E}}_n^{\text{dyn}}$ , where

$$\tilde{\mathcal{E}}_n^{\text{WP}} = \langle \overline{\Psi_{\mathbf{x}_c, \mathbf{k}_c}} | \hat{H}(t) | \overline{\Psi_{\mathbf{x}_c, \mathbf{k}_c}} \rangle, \quad (13)$$

is the wave-packet energy and

$$\tilde{\mathcal{E}}_n^{\text{dyn}} = \langle \Psi_{\mathbf{x}_c, \mathbf{k}_c}^{(0)} | i\hbar \partial_t | \Psi_{\mathbf{x}_c, \mathbf{k}_c}^{(0)} \rangle - \langle \overline{\Psi_{\mathbf{x}_c, \mathbf{k}_c}} | i\hbar \partial_t | \overline{\Psi_{\mathbf{x}_c, \mathbf{k}_c}} \rangle, \quad (14)$$

is the dynamical energy; the latter comes from the dynamical part of the definition of the Lagrangian.

By applying the principle of least action to Eq. (11), we obtain the following equations of motion for  $\mathbf{x}_c$  and  $\mathbf{k}_c$ ,

$$\hbar \dot{\mathbf{k}}_{c,i} = -eE_i, \quad (15)$$

$$\dot{\mathbf{x}}_{c,i} = \frac{1}{\hbar} \frac{\partial \tilde{\mathcal{E}}_n}{\partial k_{c,i}} + \sum_j \tilde{\Omega}_{ij}^{\mathbf{k}_c, \mathbf{k}_c} \dot{k}_{c,j} + \sum_\alpha \tilde{\Omega}_{i\alpha}^{\mathbf{k}_c, \mathbf{m}} \dot{m}_\alpha. \quad (16)$$

Here,  $\mathbf{E} = -\nabla_{\mathbf{x}_c} \phi(\mathbf{x}_c)$  is the electric field, and

$$\tilde{\Omega}_{n,i\alpha}^{\mathbf{k}_c, \mathbf{m}} = \partial_{k_{c,i}} \tilde{A}_\alpha^{\mathbf{m}} - \partial_{m_\alpha} \tilde{A}_i^{\mathbf{k}_c}, \quad (17)$$

is the Berry curvature in the  $(\mathbf{k}_c, \mathbf{m})$  phase space.  $\tilde{\Omega}_{ij}^{\mathbf{k}_c, \mathbf{k}_c}$  is the Berry curvature in the momentum space and defined in the same manner.

## III. NONLINEAR CURRENT GENERATION

### A. Dynamics under magnetic precession

Having established the formalism for the wave-packet dynamics, we now turn to studying the electric current generated by the magnetic dynamics. To this end, we consider the electrons subject to the magnetic precession of the ferromagnetic moment. Suppose the ferromagnetic moment  $\mathbf{m}(t)$  precess about  $\mathbf{m}_0$ , i.e.,  $\mathbf{m}(t) = \mathbf{m}_0 + \delta \mathbf{m}(t)$ , where  $\delta \mathbf{m}(t)$  is assumed to be small,  $\delta m \ll m_0$  ( $\delta m = |\delta \mathbf{m}(t)|$  and  $m_0 = |\mathbf{m}_0|$ ). The unperturbed term is given by  $\hat{H}^{(0)} = \hat{H}_e - J_{\text{ex}} \mathbf{m}_0 \cdot \hat{\boldsymbol{\sigma}}$ , which is composed of the electronic Hamiltonian  $\hat{H}_e$  and the exchange coupling aligned with the magnetization at the equilibrium state. Here,  $J_{\text{ex}}$  is the coupling constant between itinerant electrons and  $\mathbf{m}_0$ . The perturbation,  $\sum_\beta \delta m_\beta(t) \hat{H}'_\beta = -J_{\text{ex}} \sum_\beta \delta m_\beta(t) \hat{\sigma}_\beta$ , accounts for the exchange coupling arising from the deviation  $\delta \mathbf{m}(t)$ .

For the sake of concreteness, let us consider a magnetization precession about the  $x$ -axis with angular frequency  $\omega$ . In this case, the axis vector is  $\mathbf{m}_0 = (\sqrt{1 - (\delta m)^2}, 0, 0)^T$ , and the transverse component takes the form

$$\delta \mathbf{m}(t) = \delta \mathbf{m}^{(+)} e^{-i\omega t} + \delta \mathbf{m}^{(-)} e^{i\omega t}, \quad (18)$$

where  $\delta\mathbf{m}^{(\pm)} = \frac{\delta m}{2}(0, 1, \pm i)^T$ . For later convenience, we introduce its Fourier components

$$\delta\mathbf{m}_\Omega = \delta\mathbf{m}^{(+)}\delta_{\Omega,\omega} + \delta\mathbf{m}^{(-)}\delta_{\Omega,-\omega}. \quad (19)$$

Applying the wave packet theory in Sec. II, under the magnetization precession, we find that the wave-packet dynamics reads

$$\dot{k}_{c,i} = 0, \quad (20)$$

$$\dot{x}_{c,i} = \frac{1}{\hbar} \frac{\partial \tilde{\mathcal{E}}_n}{\partial k_{c,i}} + \sum_{\alpha} \tilde{\Omega}_{n,i\alpha}^{\mathbf{k}_c \mathbf{m}} \delta\dot{m}_\alpha. \quad (21)$$

Here,  $\delta\dot{m}_\alpha$  is the time derivative of  $\delta m_\alpha$ . In the following, we omit the subscript ‘‘c’’ in  $\mathbf{x}_c$  and  $\mathbf{k}_c$  for the sake of brevity.

### B. Choice of distribution function

The electric current is generally expressed as

$$\mathbf{j}(t) = -e \sum_n \int_{\mathbf{k}} f_n \dot{\mathbf{x}}, \quad (22)$$

where  $f_n$  is the electron distribution function for the  $n$ -th band and  $\dot{\mathbf{x}}$  denotes the wave-packet velocity given in Eq. (21). In general, the electron distribution depends on the trajectory of  $\delta\mathbf{m}(t)$  and the nature of electron scattering. The latter is caused by impurity scattering as well as electron-phonon and electron-electron interactions, encompassing both elastic and inelastic scattering processes. Such effects are well characterized by the relaxation time  $\tau$ , which measures how rapidly electrons lose the memory of their initial state. Because we are interested in the intrinsic responses, we hereafter consider the case  $\omega\tau \gg 1$ , i.e., the weak-scattering regime. In the regime  $\omega\tau \gg 1$  ( $\tau \gg T = 2\pi/\omega$ ), the driving period by magnetization precession is much shorter than the relaxation time. Therefore, the electron distribution does not change within one cycle [48].

Assuming that the perturbation is switched on adiabatically, i.e. the Hamiltonian reduces to  $\hat{H}^{(0)}$  in the initial state, the electron distribution function is taken as  $f_n = f(\mathcal{E}_n^{(0)})$  [49, 50], where  $f$  is the Fermi-Dirac distribution function [51]. Here  $\mathcal{E}_n^{(0)}$  is the energy of the  $n$ -th wave-packet in zeroth order of  $\delta m$  and reduces to the unperturbed energy  $\varepsilon_{n\mathbf{k}}^{(0)}(\mathbf{m}_0)$ . Therefore, in the situation described above, we should choose the electron distribution function as  $f_n = f(\varepsilon_{n\mathbf{k}}^{(0)}(\mathbf{m}_0))$ .

Focusing on the intrinsic response up to the second order of the perturbation, the current reads,

$$\begin{aligned} j_i(t; \mathbf{m}_0) &= -e \sum_n \int_{\mathbf{k}} f_n^{(0)} \dot{x}_{n,i} \\ &\approx -e \sum_n \int_{\mathbf{k}} f_n^{(0)} \left( \frac{1}{\hbar} \frac{\partial \mathcal{E}_n^{(2)}}{\partial k_i} + \sum_{\alpha} \Omega_{n,i\alpha}^{\mathbf{k}\mathbf{m}^{(1)}} \delta\dot{m}_\alpha(t) \right), \end{aligned} \quad (23)$$

where  $f_n^{(0)} = f(\varepsilon_{n\mathbf{k}}^{(0)}(\mathbf{m}_0))$ . Here, we explicitly denote the dependence of the precession axis  $\mathbf{m}_0$  as the SMF depends on it. In the second line, we perform the expansion  $\tilde{\mathcal{E}}_n = \sum_N \mathcal{E}_n^{(N)}$  and  $\tilde{\Omega}_{n,i\alpha}^{\mathbf{k}\mathbf{m}} = \sum_N \Omega_{n,i\alpha}^{\mathbf{k}\mathbf{m}^{(N)}}$ , where the terms with superscript  $(N)$  are in the order of  $\delta m^N$ . Equation (23) contains two contributions; the second order correction to the energy of the  $n$ -th wave-packet and the first order correction to the Berry curvature, which will be evaluated in the following section.

### C. Ingredients of nonlinear spin-motive force

The second order correction to  $\tilde{\mathcal{E}}_n$  in Eq. (23),  $\mathcal{E}_n^{(2)}$ , is obtained by substituting Eq. (10) into Eq. (13) (see Appendix.C). The result reads,

$$\begin{aligned} \mathcal{E}_n^{(2)} &= J_{\text{ex}}^2 \sum_{\alpha,\beta} \text{Re} \left[ \sum_{l(\neq n)} \frac{\varepsilon_{nl,\mathbf{k}}^{(0)}(\mathbf{m}_0) \sigma_\alpha^{nl} \sigma_\beta^{ln}}{(\varepsilon_{nl,\mathbf{k}}^{(0)}(\mathbf{m}_0))^2 - \hbar^2 \omega^2} \right] \delta m_\alpha(t) \delta m_\beta(t) \\ &+ \hbar J_{\text{ex}}^2 \sum_{\alpha,\beta} \text{Im} \left[ \sum_{l(\neq n)} \frac{\sigma_\alpha^{nl} \sigma_\beta^{ln}}{(\varepsilon_{nl,\mathbf{k}}^{(0)}(\mathbf{m}_0))^2 - \hbar^2 \omega^2} \right] \delta m_\alpha(t) \delta \dot{m}_\beta(t). \end{aligned} \quad (24)$$

On the other hand, the first order correction to the Berry curvature reads

$$\Omega_{n,i\alpha}^{\mathbf{k}\mathbf{m}^{(1)}} = \partial_{k_i} A_{n,\alpha}^{\mathbf{m}^{(1)}} - \partial_{m_\alpha} A_{n,i}^{\mathbf{k}^{(1)}}, \quad (25)$$

where

$$\begin{aligned} A_{n,i}^{\mathbf{k}^{(1)}} &= -i \langle u_{n\mathbf{k}}^{(1)}(\mathbf{m}) | \partial_{k_i} | u_{n\mathbf{k}}^{(0)}(\mathbf{m}_0) \rangle \\ &- i \langle u_{n\mathbf{k}}^{(0)}(\mathbf{m}_0) | \partial_{k_i} | u_{n\mathbf{k}}^{(1)}(\mathbf{m}) \rangle \\ &= 2\text{Re} \left[ -i \langle u_{n\mathbf{k}}^{(1)}(\mathbf{m}) | \partial_{k_i} | u_{n\mathbf{k}}^{(0)}(\mathbf{m}_0) \rangle \right], \end{aligned} \quad (26)$$

is the first order correction to the  $\mathbf{k}$ -space Berry connection for the  $n$ -th band state, and  $A_{n,\alpha}^{\mathbf{m}^{(1)}}$  is defined in the same way [52],

$$\begin{aligned} A_{n,\alpha}^{\mathbf{m}^{(1)}} &= -i \langle u_{n\mathbf{k}}^{(1)}(\mathbf{m}) | \partial_{m_\alpha} | u_{n\mathbf{k}}^{(0)}(\mathbf{m}_0) \rangle \\ &- i \langle u_{n\mathbf{k}}^{(0)}(\mathbf{m}_0) | \partial_{m_\alpha} | u_{n\mathbf{k}}^{(1)}(\mathbf{m}) \rangle \\ &= 2\text{Re} \left[ -i \langle u_{n\mathbf{k}}^{(1)}(\mathbf{m}) | \partial_{m_\alpha} | u_{n\mathbf{k}}^{(0)}(\mathbf{m}_0) \rangle \right]. \end{aligned} \quad (27)$$

Using Eq. (9), we find that the following relations hold for the first-order correction to  $\mathbf{k}$ -space and the  $\mathbf{m}$ -space Berry connection (see also Appendix.E for the derivation):

$$A_{n,\alpha}^{\mathbf{m}^{(1)}} = - \sum_{\beta} \left( \bar{\Omega}_{n,\alpha\beta}^{\mathbf{m}\mathbf{m}} \delta m_\beta(t) - 2\hbar \bar{G}_{n,\alpha\beta}^{\mathbf{m}\mathbf{m}} \delta \dot{m}_\beta(t) \right), \quad (28)$$

$$A_{n,i}^{\mathbf{k}^{(1)}} = - \sum_{\beta} \left( \bar{\Omega}_{n,i\beta}^{\mathbf{k}\mathbf{m}} \delta m_\beta(t) - 2\hbar \bar{G}_{n,i\beta}^{\mathbf{k}\mathbf{m}} \delta \dot{m}_\beta(t) \right). \quad (29)$$

Here, we introduce the ‘‘normalized’’ Berry curvature  $\bar{\Omega}_{n,\mu\nu}^{\xi\xi'}$  and Berry connection polarizability  $\bar{G}_{n,\mu\nu}^{\xi\xi'}$  for  $\xi =$

$\mathbf{k}, \mathbf{m}$ . The concrete expressions for these quantities are given in Appendix D. Substituting Eqs. (28) and (29) into Eq. (25), we find the following expression for the first-order correction to the Berry curvature,

$$\begin{aligned} \Omega_{n,i\alpha}^{\mathbf{k}\mathbf{m}(1)} &= - \sum_{\beta} \left( \partial_{k_i} \bar{\Omega}_{n,\alpha\beta}^{\mathbf{m}\mathbf{m}} - \partial_{m_\alpha} \bar{\Omega}_{n,i\beta}^{\mathbf{k}\mathbf{m}} \right) \delta m_\beta(t) \\ &\quad - 2\hbar \sum_{\beta} \left( \partial_{k_i} \bar{G}_{n,\alpha\beta}^{\mathbf{m}\mathbf{m}} - \partial_{m_\alpha} \bar{G}_{n,i\beta}^{\mathbf{k}\mathbf{m}} \right) \delta \dot{m}_\beta(t). \end{aligned} \quad (30)$$

#### D. Expressions of nonlinear spin motive force

By substituting Eqs. (24) and (30) into Eq. (23), we find that the nonlinear spin-motive force has two contributions: direct current (DC) and second harmonic generation (SHG) components,

$$j_i(t; \mathbf{m}_0) = j_i(0; \mathbf{m}_0) + 2\text{Re}[j_i(2\omega; \mathbf{m}_0)e^{-2i\omega t}]. \quad (31)$$

Here,

$$j_i(\Omega; \mathbf{m}_0) = \frac{1}{T} \int_0^T dt e^{-i\Omega t} j_i(t; \mathbf{m}_0), \quad (32)$$

is the Fourier series of the nonlinear spin-motive force along  $i$ th direction at time  $t$ ,  $j_i(t; \mathbf{m}_0)$ .

##### 1. DC term

Firstly, let us focus on the DC term which corresponds to the  $\omega = 0$  component in Eq(32). Phenomenologically, the DC component reads

$$j_i(0; \mathbf{m}_0) = \sum_{\alpha,\beta} \text{Re} \sigma_{i;\alpha\beta}(0; \omega, -\omega) \delta m_\alpha(\omega) \delta m_\beta(-\omega), \quad (33)$$

where  $\sigma_{i;\alpha\beta}(0; \omega, -\omega)$  is the nonlinear conductivity. Here, the deviation vector  $\delta \mathbf{m}(\omega)$  is considered an external field. The conductivity tensor consists of three contributions,  $\sigma_{i;\alpha\beta}(0; \omega, -\omega) = \sigma_{i;\alpha\beta}^{\text{BC}}(0; \omega, -\omega) + \sigma_{i;\alpha\beta}^{\text{BCP}}(0; \omega, -\omega) + \sigma_{i;\alpha\beta}^{\text{surf}}(0; \omega, -\omega)$ . Here, the first term is the Berry curvature-contribution,

$$\sigma_{i;\alpha\beta}^{\text{BC}}(0; \omega, -\omega) = 2ie\omega \sum_n \int_{\mathbf{k}} f_n^{(0)} \left( \partial_{k_i} \bar{\Omega}_{n,\alpha\beta}^{\mathbf{m}\mathbf{m}} - \partial_{m_\alpha} \bar{\Omega}_{n,i\beta}^{\mathbf{k}\mathbf{m}} \right), \quad (34)$$

and the second term is related to the Berry connection polarizability,

$$\begin{aligned} \sigma_{i;\alpha\beta}^{\text{BCP}}(0; \omega, -\omega) &= 4ie\hbar\omega^2 \sum_{\gamma} \sum_n \int_{\mathbf{k}} f_n^{(0)} \left( \partial_{k_i} \bar{G}_{n,\alpha\gamma}^{\mathbf{m}\mathbf{m}} - \partial_{m_\alpha} \bar{G}_{n,i\gamma}^{\mathbf{k}\mathbf{m}} \right) \epsilon_{\gamma\beta}, \end{aligned} \quad (35)$$

with  $\epsilon_{\gamma\beta}$  being the Levi-Civita epsilon tensor. The third term is a Fermi surface contribution, which reads,

$$\begin{aligned} \sigma_{i;\alpha\beta}^{\text{surf}}(0; \omega, -\omega) &= 2eJ_{\text{ex}}^2 \sum_{\substack{n,l \\ (n \neq l)}} \int_{\mathbf{k}} f_n^{(0)'} \text{Re} \left[ \frac{\epsilon_{nl,\mathbf{k}}^{(0)}(\mathbf{m}_0) v_i^{nn} \sigma_\alpha^{nl} \sigma_\beta^{ln}}{(\epsilon_{nl,\mathbf{k}}^{(0)}(\mathbf{m}_0))^2 - \hbar^2 \omega^2} \right] \end{aligned} \quad (36)$$

where  $f_n^{(0)'}$  is the energy derivative of the Fermi distribution function.

In an insulator,  $\sigma_{i;\alpha\beta}^{\text{surf}}(0; \omega, -\omega)$  does not contribute to the nonlinear spin-motive force. On the other hand, when the Fermi level crosses a band, this term seemingly gives a nonzero contribution. In the present study, we consider the limit in which electronic relaxation is much slower than the time scale of the magnetization dynamics. In realistic situations, however, a finite relaxation time is present, and this term is expected to exhibit a transient-current-like behavior, decaying within the scale of the relaxation time.

##### 2. SHG term

Next, we turn to the SHG term which is an AC response with frequency  $2\omega$  in Eq(32). This term can be written as follows,

$$j_i(2\omega; \mathbf{m}_0) = \sum_{\alpha,\beta} \sigma_{i;\alpha\beta}(2\omega; \omega, \omega) \delta m_\alpha(\omega) \delta m_\beta(\omega). \quad (37)$$

Similar to the DC term, the conductivity tensor consists of three contributions,  $\sigma_{i;\alpha\beta}(2\omega; \omega, \omega) = \sigma_{i;\alpha\beta}^{\text{BC}}(2\omega; \omega, \omega) + \sigma_{i;\alpha\beta}^{\text{BCP}}(2\omega; \omega, \omega) + \sigma_{i;\alpha\beta}^{\text{surf}}(2\omega; \omega, \omega)$ . Here,

$$\begin{aligned} \sigma_{i;\alpha\beta}^{\text{BC}}(2\omega; \omega, \omega) &= -ie\omega \sum_n \int_{\mathbf{k}} f_n^{(0)} \partial_{m_\alpha} \bar{\Omega}_{n,i\beta}^{\mathbf{k}\mathbf{m}}, \quad (38) \\ \sigma_{i;\alpha\beta}^{\text{BCP}}(2\omega; \omega, \omega) &= -2ie\hbar\omega^2 \sum_{\gamma} \sum_n \int_{\mathbf{k}} f_n^{(0)} \left( \partial_{k_i} \bar{G}_{n,\alpha\gamma}^{\mathbf{m}\mathbf{m}} - \partial_{m_\alpha} \bar{G}_{n,i\gamma}^{\mathbf{k}\mathbf{m}} \right) \epsilon_{\gamma\beta}, \end{aligned} \quad (39)$$

$$\begin{aligned} \sigma_{i;\alpha\beta}^{\text{surf}}(2\omega; \omega, \omega) &= eJ_{\text{ex}}^2 \sum_{\substack{n,l \\ (n \neq l)}} \int_{\mathbf{k}} f_n^{(0)'} \text{Re} \left[ \frac{\epsilon_{nl,\mathbf{k}}^{(0)}(\mathbf{m}_0) v_i^{nn} \sigma_\alpha^{nl} \sigma_\beta^{ln}}{(\epsilon_{nl,\mathbf{k}}^{(0)}(\mathbf{m}_0))^2 - \hbar^2 \omega^2} \right] \end{aligned} \quad (40)$$

are the Berry curvature, Berry connection polarizability, and Fermi surface contributions, respectively.

##### 3. Interpretations of results

In previous studies, currents arising from the Berry curvature have been investigated primarily in the linear regime with respect to  $\delta \mathbf{m}(t)$  in the adiabatic regime

[22, 41, 42]. It arises from using the unperturbed Berry curvature  $\Omega_n^{km(0)}$  as  $\tilde{\Omega}_n^{km}$  in Eq. (21). It is nothing but the displacement current for  $\delta\mathbf{m}(t)$  which is periodic in time. In our formalism, the contribution from  $\delta\mathbf{m}(t)$  in the perturbation theory tunes the Bloch wavefunction, and hence the expression of the Berry curvature. This leads to Eqs. (34), (38) and can be interpreted as the extension of the formula in the adiabatic regime.

The direct current induced by the Berry curvature contribution,  $\sigma^{\text{BC}}(0; \omega, -\omega)$ , is proportional to  $m_\alpha \dot{m}_\beta - m_\beta \dot{m}_\alpha$ , as  $m_\alpha \dot{m}_\beta + m_\beta \dot{m}_\alpha$  term vanishes after taking the time integral. As a consequence, the induced current is proportional to the area swept by  $\mathbf{m}(t)$ . To see this, we note that the time dependence of this contribution arises from terms proportional to the product  $m_\alpha \dot{m}_\beta$ , whose antisymmetric component,  $\mathbf{m} \times \dot{\mathbf{m}}$ , corresponds to  $\sigma^{\text{BC}}(0; \omega, -\omega)$ . In a precessional motion, the magnetization traces a closed trajectory in  $\mathbf{m}$ -space, and  $\mathbf{m} \times \dot{\mathbf{m}}$  corresponds to the area enclosed by this curve. Thus, when the magnetization dynamics forms such a closed loop, the  $\sigma^{\text{BC}}(0; \omega, -\omega)$  contribution is proportional to the area.

By contrast, the symmetric component,  $m_\alpha \dot{m}_\beta + m_\beta \dot{m}_\alpha$ , yields terms proportional to  $\cos 2\omega t$  and  $\sin 2\omega t$ , i.e., it contributes to the SHG through  $\sigma^{\text{BC}}(2\omega; \omega, \omega)$  term. Mathematically, this type of product can be written as a total time derivative,  $\frac{d}{dt}(m_\alpha m_\beta)$ . Upon integrating the current over time, one obtains a contribution of the form  $m_\alpha(t_{\text{end}})m_\beta(t_{\text{end}}) - m_\alpha(t_{\text{initial}})m_\beta(t_{\text{initial}})$ , where  $t_{\text{initial/end}}$  is beginning or end of the time integral. This term vanishes when the magnetization trajectory is closed as discussed above. On the other hand, it yields a finite value for an open trajectory, corresponding to the oscillatory components at frequency  $2\omega$ .

In addition to the Berry curvature contribution, we find contributions arising from a non-adiabatic effect (Eqs. (35) and (39)). These contributions are related to the normalized Berry connection polarizability. The dynamical correction proportional to  $\delta\dot{\mathbf{m}}(t)$  in perturbation theory is responsible for the virtual inter-band mixing for the Bloch wavefunction, which is presented in Eqs. (24) and (30). This leads to the correction beyond the adiabatic regime  $\sim \mathcal{O}(\omega)$ , which can be confirmed by the factor  $\sim \mathcal{O}(\omega^2)$  in Eqs. (35) and (39). The above discussion is analogous to the one for the intrinsic nonlinear Hall effect [28, 29]. In that situation, the electric field, the temporal dynamics of the vector potential, mixes the Bloch wavefunctions of different bands, which leads to the appearance of the the Berry connection polarizability in the  $\mathbf{k}$ -space. In our situation, the Berry connection polarizability in the  $(\mathbf{k}, \mathbf{m})$ -mixed space arises from the temporal dynamics of the magnetization.

The current arising from the Berry connection polarizability appears through the product  $\dot{m}_\alpha \dot{m}_\beta$ . For a precessing magnetization, this product explicitly takes the form  $(1 + \cos 2\omega t)$  for  $\alpha = \beta$ , or  $\sin 2\omega t$  for  $\alpha \neq \beta$ . The constant factor 1 in the former case, which corresponds to the time-averaged magnitude of the magnetization

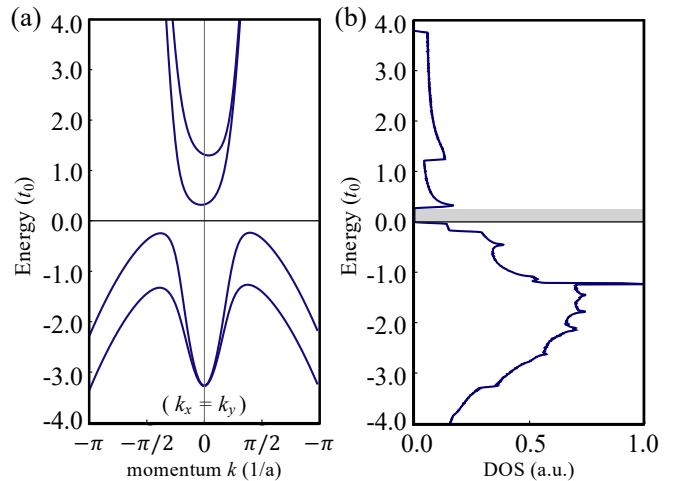


FIG. 1. (a) The band structure of  $\hat{\mathcal{H}}_{0,\mathbf{k}}$  on the  $k_x = k_y$  line. (b) Density of states. The gray shade represents energy region where band is gapped. The model parameters are set as  $\gamma_1 = 3.0t_0a^2$ ,  $\gamma_2 = 2.0t_0a^2$ ,  $\gamma_3 = 1.5t_0a^2$ ,  $\Delta = 2.0t_0$ ,  $E_R = 0.08t_0a$ ,  $E_D = 0.3t_0a$ , and  $J_c = 0.5t_0$ , where  $t_0$  is the energy unit and  $a$  is the lattice constant. The direction of the equilibrium magnetization is set along the  $x$ -direction ;  $\mathbf{m}_0 = \mathbf{e}_x$ .

dynamics, gives rise to  $\sigma^{\text{BCP}}(0; \omega, -\omega)$ , while the time-dependent deviation from it represents  $\sigma^{\text{BCP}}(2\omega; \omega, \omega)$ . The time dependence of  $\sigma^{\text{BCP}}$  is governed not so much by a geometric interpretation in terms of whether the magnetization traces a closed loop, but rather by the temporal dynamics of the magnetization itself.

## IV. LUTTINGER MODEL

### A. Hamiltonian

Now, we demonstrate the implementation of our theory in concrete materials. As an example for demonstrating the quantum geometric effect, we consider magnetic precession in a two-dimensional magnetic semiconductor. The static part of the Hamiltonian reads

$$\hat{\mathcal{H}}_{\mathbf{k}}^{(0)} = \hat{\mathcal{H}}_{\text{L}} + \hat{\mathcal{H}}_{\text{SOC}} + \hat{\mathcal{H}}_{\text{exc}}, \quad (41)$$

$$\begin{aligned} \hat{\mathcal{H}}_{\text{L}} = \frac{\gamma_1}{2} \mathbf{k}^2 + \gamma_2 \left( \frac{5}{4} \mathbf{k}^2 + \sum_{a=x,y} k_a^2 \hat{S}_a^2 \right) \\ - \gamma_3 k_x k_y \{ \hat{S}_x, \hat{S}_y \} - \Delta \left( \hat{S}_z^2 - \frac{5}{4} \right), \end{aligned} \quad (42)$$

$$\hat{\mathcal{H}}_{\text{SOC}} = E_R \left( k_x \hat{S}_y - k_y \hat{S}_x \right) + E_D \left( k_x \hat{S}_x - k_y \hat{S}_y \right), \quad (43)$$

$$\hat{\mathcal{H}}_{\text{exc}} = -J_{\text{ex}} \mathbf{m}_0 \cdot \hat{\mathbf{S}}, \quad (44)$$

where  $\mathbf{k} = (k_x, k_y)$ , and  $\hat{\mathbf{S}} = (\hat{S}_x, \hat{S}_y, \hat{S}_z)$  is the spin-3/2 operator. The first term in Eq. (41) is a variant of the

Luttinger Hamiltonian [53] where  $\gamma_{1,2,3}$  are the Luttinger parameters and  $\Delta$  is the out of plane anisotropy. The first and second terms in Eq. (43) are respectively the Rashba- and Dresselhaus-like spin-orbit couplings, which generally exist in a noncentrosymmetric system. Finally, the third term, Eq. (44), is the exchange coupling between the electrons and the local moment. Throughout this section, we set  $\gamma_1 = 3.0t_0a^2$ ,  $\gamma_2 = 2.0t_0a^2$ ,  $\gamma_3 = 1.5t_0a^2$ ,  $\Delta = 2.0t_0$ ,  $E_R = 0.08t_0a$ ,  $E_D = 0.3t_0a$ ,  $J_{\text{ex}} = 0.5t_0$ , where  $t_0$  is the energy unit and  $a$  is the lattice constant; we set  $a = 1$ , except for the order estimation of the electric current.

Figure 1 shows the dispersion along the  $k_x = k_y$  line and the density of states (DOS) of  $\hat{\mathcal{H}}_{0,\mathbf{k}}$  where the axis vector  $\mathbf{m}_0$  is aligned with the  $x$ -direction. The electronic band consists of two valence and two conduction bands; it is an indirect semiconductor with the indirect gap of  $\Delta \simeq 0.3t_0$  at around  $E = 1.2t_0$ . The gap is shown as a gray shade in Fig. 1(b).

For the effective model described above, we consider the situation where magnetization precesses around the  $x$ -axis and the nonlinear SMF generated along the  $x$ -axis. Hence, we now evaluate Eqs.(34), (35), (38), and (39) for  $i = x$  numerically.

## B. Results of numerical calculation

Figures 2(a), (b), and (c) show the results of the numerical calculation for the  $\omega$ -linear contributions to the dc current and SHG (Eqs.(34) and (38)) as a function of the Fermi energy  $E_F$ . The gray shade represents the region of  $E_F$  in which the Fermi level is in the band gap. We plot the specific energy region around the gap for the sake of visibility. In Fig. 2(a), the SMF occurs even when the Fermi level is in the energy gap, i.e., without mobile carriers. The same behavior is also observed in Figs. 2(b) and 2(c). Since this region corresponds to the insulating regime, there are no conduction electrons contributing to the current. With taking into account the appearance of the plateau in insulating regime, Figs. 2(a)-2(c) indicates that the  $\omega$ -linear term behaves in a displacement current-like manner. Figures 2(d), (e), and (f) show the results of the numerical calculation of the  $\omega$ -quadratic SMF as a function of the Fermi energy (Eqs.(35) and (39)). These numerical results also exhibit a plateau with a finite value inside the gap.

In addition, we find that, at least for the present model, the formations of the current plateau inside the gap in Fig.2 are predominantly governed by  $\bar{\Omega}_n^{km}$  or  $\bar{G}_n^{km}$ , rather than by  $\bar{\Omega}_n^{mm}$  or  $\bar{G}_n^{mm}$ . This suggests that the magnetic semiconductor described by Eq.(41) hosts the nontrivial quantum geometry in the  $(\mathbf{k}, \mathbf{m})$ -mixed space. On the other hand, this model does not have a nontrivial distribution of the Berry curvature  $\Omega_n^{kk}$  and, therefore, shows neither the anomalous Hall effect nor the finite Chern number. In that sense, this model

is a “trivial” model in the context of the conventional  $\mathbf{k}$  space-quantum geometry. Our calculations indicate that even magnetic materials which are previously regarded as quantum-geometrically trivial can exhibit non-trivial spin-charge conversions from the perspective of the  $(\mathbf{k}, \mathbf{m})$ -mixed space-quantum geometry.

	(nA/cm)		(nA/cm)
(a) : $j_x^{\text{BC}}(0; \mathbf{e}_x)$	3.62	(d) : $j_x^{\text{BCP}}(0; \mathbf{e}_x)$	-1.01
(b) : $\text{Im}[j_x^{\text{BC}}(2\omega; \mathbf{e}_x)]$	-21.1	(e) : $\text{Im}[j_x^{\text{BCP}}(2\omega; \mathbf{e}_x)]$	0.517
(c) : $\text{Re}[j_x^{\text{BC}}(2\omega; \mathbf{e}_x)]$	3.02	(f) : $\text{Re}[j_x^{\text{BCP}}(2\omega; \mathbf{e}_x)]$	-0.601

TABLE I. Summary of the values for the electric currents converted into the unit of the current density (nA/cm). In the table, (a)-(f) denote the electric currents inside the gap in the respective panels of Fig. 2. We assume that the frequency of the magnetization precession is  $\omega = 4.56 \times 10^1$  GHz.

At the end of this section, let us estimate the numerical values of the current in Fig. 2. To this end, we set the lattice constant to  $a = 10^{-7}$  cm, corresponding to the order of angstroms. The frequency is chosen as  $\hbar\omega = 0.03$  meV, which corresponds to  $\omega = 4.56 \times 10^1$  GHz. The amplitude of the magnetization precession is set to  $\delta m = 0.01$ , to ensure the validity of the perturbative treatment. The unit of energy was taken as  $t_0 = 10$  meV. With these parameters, the numerically obtained energy gap, indicated by the gray-shaded region, becomes approximately 3 meV, two orders of magnitude larger than  $\hbar\omega$ . Thus, justifying the adiabatic approximation. The current values converted under these parameter settings are summarized in Table I, which are in the order of  $10^{-1} \sim 10^1$  nA/cm. Therefore, the current induced by our mechanism can be detected on the usual current ammeter.

## V. DISCUSSION AND CONCLUSION

In this work, we theoretically proposed the intrinsic nonlinear SMF which arises from the quantum geometry in the  $(\mathbf{k}, \mathbf{m})$ -mixed space. We formulated the electron dynamics in the ferromagnets by the semiclassical wavepacket formalism up to the second order of the amplitude of the time-varying magnetization. As a result, we found that the nonlinear SMF has two contributions; the DC term and the SHG term. Both of them can be written in terms of the Berry curvature and the quantum metric in the  $(\mathbf{k}, \mathbf{m})$ -mixed. To illustrate the significance of the nonlinear SMF, we performed numerical calculations for a model of two-dimensional magnetic semiconductors. As a result, we found that, even in the insulating regime, the nonlinear SMF shows a finite value, and that value can be detected by the usual current ammeter.

The nonlinear SMF we propose is expected to exist broadly in various materials, regardless of whether they are metallic, insulating, or semiconducting. As strategies

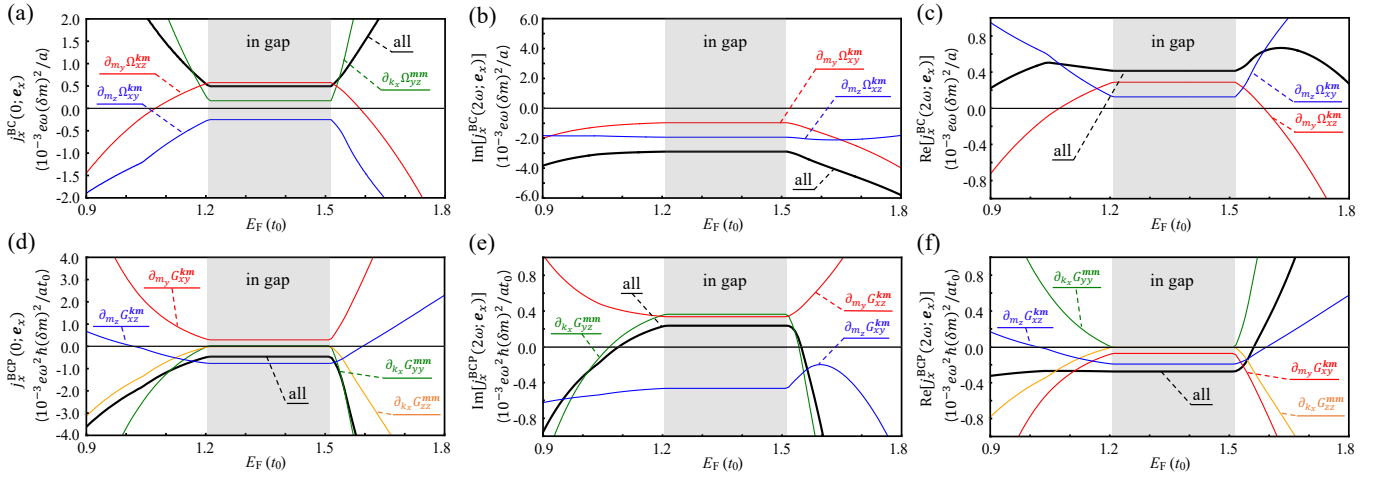


FIG. 2. Calculation results of the electric current along the  $x$ -axis under the magnetization precession around the axis  $\mathbf{m}_0 = \mathbf{e}_x$ . Upper (lower) panels show the response coefficients arising from the Berry curvature (Berry connection polarizability). Panels (a,d) show the direct-current component, while (b,e) and (c,f) show the  $\sin 2\omega t$  and  $\cos 2\omega t$  components of second-harmonic generation, respectively. The gray shade represents the energy region where the band is gapped. The colored lines in each panel represent the contributions of the geometric quantities that arise when one expands the summation for the magnetization direction,  $\alpha$  and  $\beta$ , in the expression of the electric current, Eqs. (33) and (37), explicitly.

for observing or enhancing the nonlinear SMF, we first suggest exploring materials or junction systems in which the  $(\mathbf{k}, \mathbf{m})$ -space quantum geometry is already known to exhibit a nontrivial structure, as inferred from studies on current-induced spin-orbit torques [34–36, 39]. Second, one may focus on materials with topologically nontrivial band structures or with band degeneracy points. In this sense, magnetic Weyl semimetals provide a promising platform [45] and constitute the subject of our future studies. More recently,  $\text{MnBi}_2\text{Te}_4$  has also been proposed as an intriguing candidate system [41, 54].

In our calculations, we assume that we can fix the gauge of the Berry connection in the  $\mathbf{m}$ -space to zero globally. Under this gauge condition, linear-response current, Thouless pump, does not arise. Since the main focus of this study is on nonlinear response, we intentionally restrict ourselves to situations where the Thouless pump is absent, and hence the nonlinear contribution becomes dominant. On the other hand, for materials with nontrivial band structures where a gauge cannot set the  $\mathbf{m}$ -space Berry connection to zero globally, it becomes necessary to evaluate the first-order correction to the Berry connection without relying on the above orthogonality condition. The results for such cases will be reported elsewhere [55].

Finally, we emphasize the crucial role of quantum geometry in the electric response driven by magnetization dynamics. The usefulness of the  $(\mathbf{k}, \mathbf{m})$ -mixed space quantum geometry has been discussed primarily in the

context of current-induced spin-orbit torques which is the charge-to-spin conversion [35, 38, 39]. Although preceding studies have shown that the reciprocal process, SMF, is written by the Berry curvature in mixed space, it is limited to the linear response regime and hence AC. It was also unknown how the quantum metric affects the conversion process from the magnetic dynamics to electric current. Our study demonstrates that the SMF in the nonlinear regime can convert injected frequency into DC rectification and SHG, and their geometric origins are distinguished by their frequency scaling. This suggests that our mechanism serves as a new operating principle for an AC-to-DC converter, governed solely by the electron's geometric property in magnetic materials. Our finding not only forms the basis for exploring rich intrinsic nonlinear electric responses in dynamical magnetic systems, but also serves as a building block for the emerging field of nonlinear spintronics.

## ACKNOWLEDGMENTS

The authors thank Naoto Nagaosa, Shuichi Murakami, and Takahiro Morimoto for fruitful discussions. This work was supported by JST SPRING, Grant No. JPMJSP2136 (T.M.), JSPS KAKENHI, Grant No. JP25H00841 (H.I.), JP25H01250 (K.N.), and JST PRESTO, Grant No. JPMJPR2452 (H.I.).

[1] J. Sinova, S. O. Valenzuela, J. Wunderlich, C. H. Back, and T. Jungwirth, Spin Hall effects, *Rev. Mod. Phys.* **87**,

- [2] E. Saitoh, S. Maekawa, S. O. Valenzuela, and T. Kimura, *Spin current* (Oxford University Press, 2017).
- [3] A. Manchon, J. Železný, I. M. Miron, T. Jungwirth, J. Sinova, A. Thiaville, K. Garello, and P. Gambardella, Current-induced spin-orbit torques in ferromagnetic and antiferromagnetic systems, *Rev. Mod. Phys.* **91**, 035004 (2019).
- [4] S. E. Barnes and S. Maekawa, Generalization of faraday's law to include nonconservative spin forces, *Phys. Rev. Lett.* **98**, 246601 (2007).
- [5] R. A. Duine, Spin pumping by a field-driven domain wall, *Phys. Rev. B* **77**, 014409 (2008).
- [6] Y. Tserkovnyak and M. Mecklenburg, Electron transport driven by nonequilibrium magnetic textures, *Phys. Rev. B* **77**, 134407 (2008).
- [7] S. A. Yang, G. S. D. Beach, C. Knutson, D. Xiao, Q. Niu, M. Tsoi, and J. L. Erskine, Universal electromotive force induced by domain wall motion, *Phys. Rev. Lett.* **102**, 067201 (2009).
- [8] J. Shibata and H. Kohno, Spin and charge transport induced by gauge fields in a ferromagnet, *Phys. Rev. B* **84**, 184408 (2011).
- [9] R. Cheng and Q. Niu, Electron dynamics in slowly varying antiferromagnetic texture, *Phys. Rev. B* **86**, 245118 (2012).
- [10] J.-i. Ohe and Y. Shimada, Cascaded spin motive force driven by the dynamics of the skyrmion lattice, *Applied Physics Letters* **103** (2013).
- [11] Y. Shimada and J.-i. Ohe, Spin motive force driven by skyrmion dynamics in magnetic nanodisks, *Phys. Rev. B* **91**, 174437 (2015).
- [12] K. M. D. Hals and A. Brataas, Spin-motive forces and current-induced torques in ferromagnets, *Phys. Rev. B* **91**, 214401 (2015).
- [13] Y. Yamane and J. Ieda, Skyrmion-generated spinmotive forces in inversion broken ferromagnets, *Journal of Magnetism and Magnetic Materials* **491**, 165550 (2019).
- [14] P. N. Hai, S. Ohya, M. Tanaka, S. E. Barnes, and S. Maekawa, Electromotive force and huge magnetoresistance in magnetic tunnel junctions, *Nature* **458**, 489 (2009).
- [15] Y. Yamane, K. Sasage, T. An, K. Harii, J.-i. Ohe, J. Ieda, S. E. Barnes, E. Saitoh, and S. Maekawa, Continuous generation of spinmotive force in a patterned ferromagnetic film, *Physical review letters* **107**, 236602 (2011).
- [16] T. Schulz, R. Ritz, A. Bauer, M. Halder, M. Wagner, C. Franz, C. Pfleiderer, K. Everschor, M. Garst, and A. Rosch, Emergent electrodynamics of skyrmions in a chiral magnet, *Nature Physics* **8**, 301 (2012).
- [17] M. Hayashi, J. Ieda, Y. Yamane, J.-i. Ohe, Y. K. Takahashi, S. Mitani, and S. Maekawa, Time-domain observation of the spinmotive force in permalloy nanowires, *Physical review letters* **108**, 147202 (2012).
- [18] K. Tanabe, D. Chiba, J. Ohe, S. Kasai, H. Kohno, S. Barnes, S. Maekawa, K. Kobayashi, and T. Ono, Spin-motive force due to a gyrating magnetic vortex, *Nature communications* **3**, 845 (2012).
- [19] K.-W. Kim, J.-H. Moon, K.-J. Lee, and H.-W. Lee, Prediction of giant spin motive force due to rashba spin-orbit coupling, *Physical review letters* **108**, 217202 (2012).
- [20] G. Tatara, N. Nakabayashi, and K.-J. Lee, Spin motive force induced by rashba interaction in the strong *sd* coupling regime, *Phys. Rev. B* **87**, 054403 (2013).
- [21] Y. Yamane, J. Ieda, and S. Maekawa, Spinmotive force with static and uniform magnetization induced by a time-varying electric field, *Phys. Rev. B* **88**, 014430 (2013).
- [22] F. Freimuth, S. Blügel, and Y. Mokrousov, Direct and inverse spin-orbit torques, *Phys. Rev. B* **92**, 064415 (2015).
- [23] D. Xiao, M.-C. Chang, and Q. Niu, Berry phase effect on electronic properties, *Rev. Mod. Phys.* **82**, 1959 (2010).
- [24] N. Nagaosa, J. Sinova, S. Onoda, A. H. MacDonald, and N. P. Ong, Anomalous Hall effect, *Rev. Mod. Phys.* **82**, 1539 (2010).
- [25] A. Bandyopadhyay, N. B. Joseph, and A. Narayan, Non-linear hall effects: Mechanisms and materials, *Materials Today Electronics* **8**, 100101 (2024).
- [26] T. Liu, X.-B. Qiang, H.-Z. Lu, and X. Xie, Quantum geometry in condensed matter, *National Science Review* **12**, nwae334 (2025).
- [27] A. Gao, N. Nagaosa, N. Ni, and S.-Y. Xu, Quantum geometry phenomena in condensed matter systems, *arXiv preprint arXiv:2508.00469* (2025).
- [28] Y. Gao, S. A. Yang, and Q. Niu, Field induced positional shift of bloch electrons and its dynamical implications, *Physical review letters* **112**, 166601 (2014).
- [29] I. Sodemann and L. Fu, Quantum nonlinear hall effect induced by berry curvature dipole in time-reversal invariant materials, *Physical review letters* **115**, 216806 (2015).
- [30] C. Xiao, Z. Du, and Q. Niu, Theory of nonlinear hall effects: Modified semiclassics from quantum kinetics, *Physical Review B* **100**, 165422 (2019).
- [31] Y. Zhang and L. Fu, Terahertz detection based on nonlinear hall effect without magnetic field, *Proceedings of the National Academy of Sciences* **118**, e2100736118 (2021).
- [32] B. Cheng, Y. Gao, Z. Zheng, S. Chen, Z. Liu, L. Zhang, Q. Zhu, H. Li, L. Li, and C. Zeng, Giant nonlinear hall and wireless rectification effects at room temperature in the elemental semiconductor tellurium, *Nature Communications* **15**, 5513 (2024).
- [33] Y. Onishi and L. Fu, High-efficiency energy harvesting based on a nonlinear hall rectifier, *Phys. Rev. B* **110**, 075122 (2024).
- [34] H. Kurebayashi, J. Sinova, D. Fang, A. Irvine, T. Skinner, J. Wunderlich, V. Novák, R. Campion, B. Gallagher, E. Vehstedt, et al., An antidamping spin-orbit torque originating from the Berry curvature, *Nature nanotechnology* **9**, 211 (2014).
- [35] F. Freimuth, S. Blügel, and Y. Mokrousov, Spin-orbit torques in Co/Pt(111) and Mn/W(001) magnetic bilayers from first principles, *Phys. Rev. B* **90**, 174423 (2014).
- [36] J.-P. Hanke, F. Freimuth, C. Niu, S. Blügel, and Y. Mokrousov, Mixed weyl semimetals and low-dissipation magnetization control in insulators by spin-orbit torques, *Nature Communications* **8**, 1479 (2017).
- [37] B. Xiong, H. Chen, X. Li, and Q. Niu, Electronic contribution to the geometric dynamics of magnetization, *Phys. Rev. B* **98**, 035123 (2018).
- [38] C. Xiao, B. Xiong, and Q. Niu, Electric driving of magnetization dynamics in a hybrid insulator, *Phys. Rev. B* **104**, 064433 (2021).
- [39] C. Xiao, H. Liu, W. Wu, H. Wang, Q. Niu, and S. A. Yang, Intrinsic nonlinear electric spin generation in centrosymmetric magnets, *Phys. Rev. Lett.* **129**, 086602 (2022).
- [40] C. Xiao, W. Wu, H. Wang, Y.-X. Huang, X. Feng, H. Liu, G.-Y. Guo, Q. Niu, and S. A. Yang, Time-reversal-even nonlinear current induced spin polarization, *Phys. Rev.*

- Lett. **130**, 166302 (2023).
- [41] J. Tang and R. Cheng, Lossless spin-orbit torque in anti-ferromagnetic topological insulator  $\text{mnbi}_2\text{te}_4$ , Phys. Rev. Lett. **132**, 136701 (2024).
- [42] A. Manchon and A. Pezo, Charge pumping with strong spin-orbit coupling: Fermi surface breathing, berry curvature, and higher harmonic generation, Phys. Rev. B **109**, 184409 (2024).
- [43] X. Feng, W. Wu, H. Wang, W. Gao, L. K. Ang, Y. Zhao, C. Xiao, and S. A. Yang, Quantum metric nonlinear spin-orbit torque enhanced by topological bands, Materials Today Quantum , 100040 (2025).
- [44] Y. Ren, W. Chen, C. Wang, T. Cao, and D. Xiao, Adiabatic pumping of orbital magnetization by spin precession, Phys. Rev. Lett. **134**, 176702 (2025).
- [45] T. Meguro, A. Ozawa, K. Kobayashi, Y. Araki, and K. Nomura, Topological spin-orbit torque in ferrimagnetic weyl semimetal, Physical Review Research **7**, L022065 (2025).
- [46] G. Sundaram and Q. Niu, Wave-packet dynamics in slowly perturbed crystals: Gradient corrections and berry-phase effects, Phys. Rev. B **59**, 14915 (1999).
- [47] One can consider the Hamiltonian has  $\mathbf{x}_c$ -dependencies other than the electrostatic potential, such as vector potential and lattice distortion. In this situation, we define the local Hamiltonian and a gradient one by expanding the Hamiltonian around  $\mathbf{x}_c$ ;  $\hat{H}^{(0)} = \hat{H}_c^{(0)} + \Delta\hat{H}^{(0)}$  where  $\hat{H}_c^{(0)}$  only contains  $\mathbf{x}_c$ , and  $\Delta\hat{H}^{(0)}$  contains the power of the spatial gradient  $\partial_{\mathbf{x}_c}$ . Because of the length scale of the modulation field mentioned above,  $\hat{H}_c^{(0)}$  is lattice periodic locally, and therefore we can obtain its Bloch eigenstates and values at each point  $\mathbf{x}_c$  locally.
- [48] A. Harada and H. Ishizuka, Spin motive force by the momentum-space berry phase in magnetic weyl semimetals, Phys. Rev. B **107**, 195202 (2023).
- [49] H. Ishizuka, T. Hayata, M. Ueda, and N. Nagaosa, Emergent electromagnetic induction and adiabatic charge pumping in noncentrosymmetric weyl semimetals, Phys. Rev. Lett. **117**, 216601 (2016).
- [50] H. Ishizuka, T. Hayata, M. Ueda, and N. Nagaosa, Momentum-space electromagnetic induction in weyl semimetals, Phys. Rev. B **95**, 245211 (2017).
- [51] In contrast, in the regime  $\omega\tau \ll 1$ , electrons undergo repeated scattering during one cycle, therefore the ex-

trinsic response dominates. In this situation, the system does not retain memory of the past distribution, and therefore each moment can be regarded as a local equilibrium. Consequently, the appropriate distribution function is  $f(\tilde{\varepsilon}_n)$ , where  $\tilde{\varepsilon}_n$  is the eigenvalues of the total Hamiltonian  $\hat{H}(t) = \hat{H}^{(0)} + \delta m_\beta(t)\hat{H}'_\beta$ .

- [52] In our calculations, the first-order correction to the Berry connection is evaluated by using the orthogonality relation between eigenstates  $\langle u_{n\mathbf{k}}^{(1)}(\mathbf{m}) | u_{n\mathbf{k}}^{(0)}(\mathbf{m}_0) \rangle = 0$ , which corresponds to fixing the gauge such that the Berry connection in the  $\mathbf{m}$ -space is zero.
- [53] J. M. Luttinger, Quantum theory of cyclotron resonance in semiconductors: General theory, Phys. Rev. **102**, 1030 (1956).
- [54] J.-X. Qiu, B. Ghosh, J. Schütte-Engel, T. Qian, M. Smith, Y.-T. Yao, J. Ahn, Y.-F. Liu, A. Gao, C. Tzschaschel, et al., Observation of the axion quasiparticle in 2d  $\text{mnbi}_2\text{te}_4$ , Nature , 1 (2025).
- [55] T. Meguro, H. Ishizuka, and K. Nomura, in preparation.
- [56] E. I. Blount, in Solid State Physics, edited by F. Seitz and D. Turnbull Academic Press, New York, 1962 , Vol. 13, p. 305.

## APPENDIX

### Appendix A: Derivation of the correction to the wave function

Firstly, let us derive the differential equation for the coefficients  $C_{l\mathbf{k}}(\mathbf{x}_c, \mathbf{k}_c, t)$ . Hereafter, we omit  $(\mathbf{x}_c, \mathbf{k}_c, t)$ -dependence of the coefficients for notational simplicity. The wave-packet follows the time-dependent Schrödinger equation.

$$i\hbar\partial_t |\Psi_{\mathbf{x}_c, \mathbf{k}_c}\rangle = \left( \hat{H}^{(0)} + \hat{V}(t) \right) |\Psi_{\mathbf{x}_c, \mathbf{k}_c}\rangle, \quad (\text{A1})$$

where  $\hat{V}(t) = \sum_\beta \delta m_\beta(t)\hat{H}'_\beta$ . Substituting the wave-packet wavefunction, Eq. (3), into Eq. (A1), and multiplying the Bloch eigenstate  $\langle \psi_{m\mathbf{k}'}^{(0)}(\mathbf{m}_0) |$  on both sides of the equation, we get the following differential equation,

$$i\hbar\partial_t C_{n\mathbf{k}}\delta_{mn} + i\hbar \sum_{l \neq n} \partial_t C_{l\mathbf{k}}\delta_{ml} = \varepsilon_{n\mathbf{k}}^{(0)}(\mathbf{x}_c, \mathbf{m}_0)C_{n\mathbf{k}}\delta_{mn} + \sum_{l(\neq n)} \varepsilon_{l\mathbf{k}}^{(0)}(\mathbf{x}_c, \mathbf{m}_0)C_{l\mathbf{k}}\delta_{ml} + (\hat{V}(t))_{ln}C_{n\mathbf{k}} + \sum_{l(\neq n)} (\hat{V}(t))_{ml}C_{l\mathbf{k}}, \quad (\text{A2})$$

Here, we use the orthogonal relation,  $\langle u_{m\mathbf{k}'}^{(0)}(\mathbf{m}_0) | u_{n\mathbf{k}}^{(0)}(\mathbf{m}_0) \rangle = \delta(\mathbf{k} - \mathbf{k}')\delta_{mn}$ . One can

separate Eq.(A2) into the intra-band contribution and inter-band contribution ( $m \neq n$ ),

$$i\hbar\partial_t C_{n\mathbf{k}} = \varepsilon_{n\mathbf{k}}^{(0)}(\mathbf{x}_c, \mathbf{m}_0)C_{n\mathbf{k}} + (\hat{V}(t))_{nn}C_{n\mathbf{k}} + \sum_{l(\neq n)} (\hat{V}(t))_{nl}C_{l\mathbf{k}}, \quad (\text{A3})$$

$$i\hbar\partial_t C_{m\mathbf{k}} = \varepsilon_{m\mathbf{k}}^{(0)}(\mathbf{x}_c, \mathbf{m}_0)C_{m\mathbf{k}} + (\hat{V}(t))_{mn}C_{n\mathbf{k}} + \sum_{l(\neq n)} (\hat{V}(t))_{ml}C_{l\mathbf{k}}. \quad (\text{A4})$$

We need to solve the second differential equation, Eq. (A4). To proceed, we assume that  $C_{l\mathbf{k}}$  for  $l \neq n$  differs from  $C_{n\mathbf{k}}$  only by an overall factor  $M_{ln,\mathbf{k}}$ ,

$$C_{l\mathbf{k}} = M_{ln,\mathbf{k}} C_{n\mathbf{k}}. \quad (\text{A5})$$

Then, substituting Eq.(A5) into Eq.(A4), and after straightforward algebra, we arrive at

$$i\hbar\partial_t M_{ln,\mathbf{k}} = \varepsilon_{ln,\mathbf{k}}^{(0)}(\mathbf{x}_c, \mathbf{m}_0)M_{ln,\mathbf{k}} + (\hat{V}(t))_{ln} - (\hat{V}(t))_{nn}M_{ln,\mathbf{k}} + \sum_{m(\neq n)} (\hat{V}(t))_{lm}M_{mn,\mathbf{k}} - \sum_{m(\neq n)} M_{ln,\mathbf{k}}(\hat{V}(t))_{nm}M_{mn,\mathbf{k}}, \quad (\text{A6})$$

The coefficient  $M_{ln,\mathbf{k}}$  is expanded in powers of the precession amplitude as  $M_{ln,\mathbf{k}} = \sum_{N \geq 1} M_{ln,\mathbf{k}}^{(N)}$ , and  $M_{ln,\mathbf{k}}^{(N)} \propto \mathcal{O}(\delta m^N)$ . Noting that  $\hat{H}'_\beta$  is already  $\mathcal{O}(\delta m^1)$ , the differential equation for  $M_{ln,\mathbf{k}}^{(1)}$  reads,

$$i\hbar\partial_t M_{ln,\mathbf{k}}^{(1)} = \varepsilon_{ln,\mathbf{k}}^{(0)}(\mathbf{x}_c, \mathbf{m}_0)M_{ln,\mathbf{k}}^{(1)} + (\hat{V}(t))_{ln}. \quad (\text{A7})$$

Employing the Fourier transformations for the time-

varying magnetization and  $M_{ln,\mathbf{k}}^{(1)}$ ,

$$\delta\mathbf{m}(t) = \sum_{\Omega} \delta m_{\Omega} e^{-i\Omega t}, \quad (\text{A8})$$

$$M_{ln,\mathbf{k}}^{(1)}(\mathbf{x}_c, \mathbf{k}_c, t) = \sum_{\Omega} M_{ln,\mathbf{k}}^{(1)}(\mathbf{x}_c, \mathbf{k}_c, \Omega) e^{-i\Omega t} \quad (\text{A9})$$

we find that the solution of Eq.(A7) reads,

$$M_{ln,\mathbf{k}}^{(1)}(\mathbf{x}_c, \mathbf{k}_c, t) = - \sum_{\Omega} \frac{\delta m_{\Omega,\beta} e^{-i\Omega t}}{\varepsilon_{ln,\mathbf{k}}^{(0)}(\mathbf{x}_c, \mathbf{m}_0) - \hbar\Omega} (\hat{H}'_\beta)_{ln}. \quad (\text{A10})$$

## Appendix B: Derivation of Eq. (12)

The Lagrangian is defined as

$$L = \langle \overline{\Psi_{\mathbf{x}_c, \mathbf{k}_c}} | \left( i\hbar \frac{d}{dt} - \hat{H}(t) \right) | \overline{\Psi_{\mathbf{x}_c, \mathbf{k}_c}} \rangle. \quad (\text{B1})$$

The time-dependencies are included in the coefficients  $C_{n\mathbf{k}}$  of the wave-packet and the perturbation-included Bloch states  $|\tilde{u}_{n\mathbf{k}}(\mathbf{x}_c, \mathbf{m})\rangle$ . Hence, we can expand the total derivative with respect to time and separate the terms as follow,

$$\begin{aligned} L &= \langle \overline{\Psi_{\mathbf{x}_c, \mathbf{k}_c}} | i\hbar\partial_t | \overline{\Psi_{\mathbf{x}_c, \mathbf{k}_c}} \rangle + i\hbar\dot{\mathbf{m}} \cdot \langle \overline{\Psi_{\mathbf{x}_c, \mathbf{k}_c}} | \partial_{\mathbf{m}} | \overline{\Psi_{\mathbf{x}_c, \mathbf{k}_c}} \rangle - \langle \overline{\Psi_{\mathbf{x}_c, \mathbf{k}_c}} | \hat{H}(t) | \overline{\Psi_{\mathbf{x}_c, \mathbf{k}_c}} \rangle \\ &= \langle \overline{\Psi_{\mathbf{x}_c, \mathbf{k}_c}}^{(0)} | i\hbar\partial_t | \overline{\Psi_{\mathbf{x}_c, \mathbf{k}_c}}^{(0)} \rangle + i\hbar\dot{\mathbf{m}} \cdot \langle \overline{\Psi_{\mathbf{x}_c, \mathbf{k}_c}} | \partial_{\mathbf{m}} | \overline{\Psi_{\mathbf{x}_c, \mathbf{k}_c}} \rangle \\ &\quad - \left( \langle \overline{\Psi_{\mathbf{x}_c, \mathbf{k}_c}}^{(0)} | i\hbar\partial_t | \overline{\Psi_{\mathbf{x}_c, \mathbf{k}_c}}^{(0)} \rangle - \langle \overline{\Psi_{\mathbf{x}_c, \mathbf{k}_c}} | i\hbar\partial_t | \overline{\Psi_{\mathbf{x}_c, \mathbf{k}_c}} \rangle + \langle \overline{\Psi_{\mathbf{x}_c, \mathbf{k}_c}} | \hat{H}(t) | \overline{\Psi_{\mathbf{x}_c, \mathbf{k}_c}} \rangle \right) \end{aligned} \quad (\text{B2})$$

where we neglect the derivative with respect to  $\mathbf{x}_c$  because, under the approximation that discards terms of order  $(\delta m \nabla_{\mathbf{x}_c})$  and higher, it is not essential for the present analysis. The third to the fifth terms in Eq.(B2) are the wave-packet energy  $\tilde{\mathcal{E}}_n$  and evaluated in Appendix.C.

The first term in Eq.(B2) can read as follow by using the phase factor of the coefficient  $C_{n\mathbf{k}}$ ;  $C_{n\mathbf{k}} =$

$$|C_{n\mathbf{k}}| e^{-i\gamma_{n\mathbf{k}}},$$

$$\begin{aligned} &\langle \overline{\Psi_{\mathbf{x}_c, \mathbf{k}_c}}^{(0)} | i\hbar\partial_t | \overline{\Psi_{\mathbf{x}_c, \mathbf{k}_c}}^{(0)} \rangle \\ &= i\hbar \int_{\mathbf{k}} |C_{n\mathbf{k}}| \partial_t |C_{n\mathbf{k}}| + \hbar \int_{\mathbf{k}} |C_{n\mathbf{k}}|^2 \partial_t \gamma_{n\mathbf{k}} \\ &= \hbar \partial_t \gamma_{n\mathbf{k}_c} \\ &= \hbar \frac{d}{dt} \gamma_{n\mathbf{k}_c} - \hbar \dot{\mathbf{k}}_c \cdot \partial_{\mathbf{k}_c} \gamma_{n\mathbf{k}_c} - \hbar \dot{\mathbf{x}}_c \cdot \partial_{\mathbf{x}_c} \gamma_{n\mathbf{k}_c} \end{aligned} \quad (\text{B3})$$

In the second line of Eq.(B3), we use the normalization condition for the coefficient;  $\int_{\mathbf{k}} |C_{n\mathbf{k}}|^2 = 1 -$

$\sum_{l(\neq n)} \int_{\mathbf{k}} |C_{l\mathbf{k}}|^2 \approx 1$ . In the following, we ignore the third term in the last line of Eq.(B3) by assuming the approximation described above. The second term of the third line in Eq.(B3) can be rewritten by using the condition  $\mathbf{x}_c = \langle \Psi_{\mathbf{x}_c, \mathbf{k}_c} | \hat{\mathbf{x}} | \Psi_{\mathbf{x}_c, \mathbf{k}_c} \rangle$  as follows. Substituting the wave-packet wavefunction and using the expression of the matrix elements of the position operator [56]

$$\langle \psi_{n\mathbf{q}}^{(0)} | \hat{\mathbf{x}} | \psi_{n'\mathbf{q}'}^{(0)} \rangle = \left\{ i \frac{\partial}{\partial \mathbf{q}} \delta_{nn'} + \langle u_{n\mathbf{q}}^{(0)} | i \partial_{\mathbf{q}} | u_{n'\mathbf{q}'}^{(0)} \rangle \right\} \delta(\mathbf{q} - \mathbf{q}'), \quad (\text{B4})$$

we find that this condition can read

$$\mathbf{x}_c = \partial_{\mathbf{k}_c} \gamma_{n\mathbf{k}_c} - \tilde{\mathbf{A}}_n^{\mathbf{k}_c}, \quad (\text{B5})$$

where the perturbation-included Berry connections in the momentum space are introduced as  $\tilde{\mathbf{A}}_n^{\mathbf{k}_c} = -i \langle \tilde{u}_{n\mathbf{k}_c}(\mathbf{x}_c, \mathbf{m}) | \partial_{\mathbf{k}_c} | \tilde{u}_{n\mathbf{k}_c}(\mathbf{x}_c, \mathbf{m}) \rangle$ . Hence Eq.(B3) eventually reads

$$\begin{aligned} & \langle \Psi_{\mathbf{x}_c, \mathbf{k}_c}^{(0)} | i \hbar \partial_t | \Psi_{\mathbf{x}_c, \mathbf{k}_c}^{(0)} \rangle \\ &= \hbar \frac{d}{dt} \gamma_{n\mathbf{k}_c} - \hbar \dot{\mathbf{k}}_c \cdot (\mathbf{x}_c + \tilde{\mathbf{A}}_n^{\mathbf{k}_c}) \\ &= \hbar \frac{d}{dt} (\gamma_{n\mathbf{k}_c} - \mathbf{x}_c \cdot \mathbf{k}_c) + \hbar \dot{\mathbf{x}}_c \cdot \mathbf{k}_c - \hbar \dot{\mathbf{k}}_c \cdot \tilde{\mathbf{A}}_n^{\mathbf{k}_c}. \end{aligned} \quad (\text{B6})$$

On the other hand, the second term in Eq.(B2) is expressed by introducing the perturbation-included Berry connection in the magnetization space  $\tilde{\mathbf{A}}_n^{\mathbf{m}} = -i \langle \tilde{u}_{n\mathbf{k}_c}(\mathbf{x}_c, \mathbf{m}) | \partial_{\mathbf{m}} | \tilde{u}_{n\mathbf{k}_c}(\mathbf{x}_c, \mathbf{m}) \rangle$ ,

$$i \hbar \dot{\mathbf{m}} \cdot \langle \overline{\Psi_{\mathbf{x}_c, \mathbf{k}_c}} | \partial_{\mathbf{m}} | \overline{\Psi_{\mathbf{x}_c, \mathbf{k}_c}} \rangle = -\hbar \dot{\mathbf{m}} \cdot \tilde{\mathbf{A}}_n^{\mathbf{m}} \quad (\text{B7})$$

If the electrostatic potential contained in the static Hamiltonian is written explicitly as a separate term, then by combining Eqs. (B6) and (B7), the Lagrangian can finally be written as the form of Eq.(12) in the main text.

### Appendix C: Derivation of Eq. (24)

Here we derive the wave-packet energy up to the order of  $\delta m^2$ . Its definition is as follow,

$$\tilde{\mathcal{E}}_n = \tilde{\mathcal{E}}_n^{\text{WP}} + \tilde{\mathcal{E}}_n^{\text{dyn}}, \quad (\text{C1})$$

$$\tilde{\mathcal{E}}_n^{\text{WP}} = \langle \overline{\Psi_{\mathbf{x}_c, \mathbf{k}_c}} | \hat{H}(t) | \overline{\Psi_{\mathbf{x}_c, \mathbf{k}_c}} \rangle, \quad (\text{C2})$$

$$\tilde{\mathcal{E}}_n^{\text{dyn}} = \langle \Psi_{\mathbf{x}_c, \mathbf{k}_c}^{(0)} | i \hbar \partial_t | \Psi_{\mathbf{x}_c, \mathbf{k}_c}^{(0)} \rangle - \langle \overline{\Psi_{\mathbf{x}_c, \mathbf{k}_c}} | i \hbar \partial_t | \overline{\Psi_{\mathbf{x}_c, \mathbf{k}_c}} \rangle. \quad (\text{C3})$$

Substituting the Hamiltonian and the wave-packet wavefunction into Eq.(C2) and summing the terms up to the second-order of perturbation, we find the following expression,

$$\begin{aligned} \mathcal{E}_n^{\text{WP}(2)} &= 2\delta \langle \Psi_{\mathbf{x}_c, \mathbf{k}_c}^{(0)} | \hat{H}^{(0)} | \Psi_{\mathbf{x}_c, \mathbf{k}_c}^{(0)} \rangle + \langle \Psi_{\mathbf{x}_c, \mathbf{k}_c}^{(1)} | \hat{H}^{(0)} | \Psi_{\mathbf{x}_c, \mathbf{k}_c}^{(1)} \rangle \\ &+ \sum_{\beta} 2\text{Re} \left[ \langle \Psi_{\mathbf{x}_c, \mathbf{k}_c}^{(0)} | \delta m_{\beta}(t) \hat{H}'_{\beta} | \Psi_{\mathbf{x}_c, \mathbf{k}_c}^{(1)} \rangle \right] \end{aligned} \quad (\text{C4})$$

The first line in Eq.(C4) can be rewritten as

$$\begin{aligned} & 2\delta \langle \Psi_{\mathbf{x}_c, \mathbf{k}_c}^{(0)} | \hat{H}^{(0)} | \Psi_{\mathbf{x}_c, \mathbf{k}_c}^{(0)} \rangle + \langle \Psi_{\mathbf{x}_c, \mathbf{k}_c}^{(1)} | \hat{H}^{(0)} | \Psi_{\mathbf{x}_c, \mathbf{k}_c}^{(1)} \rangle \\ &= \sum_{l(\neq n)} \varepsilon_{ln}^{(0)}(\mathbf{x}_c, \mathbf{m}_0) M_{ln, \mathbf{k}_c}^{(1)*} M_{ln, \mathbf{k}_c}^{(1)}, \end{aligned} \quad (\text{C5})$$

while the second line in Eq.(C4) can be rewritten by substituting the wave-packet wavefunction

$$\begin{aligned} & \sum_{\beta} 2\text{Re} \left[ \langle \Psi_{\mathbf{x}_c, \mathbf{k}_c}^{(0)} | \delta m_{\beta}(t) \hat{H}'_{\beta} | \Psi_{\mathbf{x}_c, \mathbf{k}_c}^{(1)} \rangle \right] \\ &= \sum_{\beta} 2\text{Re} \left[ \int_{\mathbf{k}} \int_{\mathbf{k}'} C_{n\mathbf{k}}^* \sum_{l(\neq n)} M_{ln, \mathbf{k}'}^{(1)} C_{n\mathbf{k}'} \right. \\ &\quad \left. \times \langle \psi_{n\mathbf{k}}^{(0)}(\mathbf{m}_0) | \delta m_{\beta}(t) \hat{H}'_{\beta} | \psi_{l\mathbf{k}'}^{(0)}(\mathbf{m}_0) \rangle \right] \\ &= \sum_{\beta} 2\text{Re} \left[ \sum_{l(\neq n)} M_{ln, \mathbf{k}_c}^{(1)} (\hat{H}'_{\beta})_{ln} \right] \delta m_{\beta}(t). \end{aligned} \quad (\text{C6})$$

On the other hand, the dynamical energy is calculated up to the second-order as follow,

$$\begin{aligned} \mathcal{E}_n^{\text{dyn}(2)} &= -\delta \langle \Psi_{\mathbf{x}_c, \mathbf{k}_c}^{(0)} | i \hbar \partial_t | \Psi_{\mathbf{x}_c, \mathbf{k}_c}^{(0)} \rangle - \langle \Psi_{\mathbf{x}_c, \mathbf{k}_c}^{(0)} | (i \hbar \partial_t \delta) | \Psi_{\mathbf{x}_c, \mathbf{k}_c}^{(0)} \rangle \\ &- \langle \Psi_{\mathbf{x}_c, \mathbf{k}_c}^{(1)} | i \hbar \partial_t | \Psi_{\mathbf{x}_c, \mathbf{k}_c}^{(1)} \rangle. \end{aligned} \quad (\text{C7})$$

The first line in Eq.(C7) can be expressed as follow by substituting the wave-packet wavefunction,

$$\begin{aligned} & -\delta \langle \Psi_{\mathbf{x}_c, \mathbf{k}_c}^{(0)} | i \hbar \partial_t | \Psi_{\mathbf{x}_c, \mathbf{k}_c}^{(0)} \rangle - \langle \Psi_{\mathbf{x}_c, \mathbf{k}_c}^{(0)} | (i \hbar \partial_t \delta) | \Psi_{\mathbf{x}_c, \mathbf{k}_c}^{(0)} \rangle \\ &= -2\hbar \delta \partial_t \gamma_{n\mathbf{k}_c} - i \hbar \partial_t \delta. \end{aligned} \quad (\text{C8})$$

The second line is somewhat complicated but can be expressed by some algebras,

$$\begin{aligned} & \langle \Psi_{\mathbf{x}_c, \mathbf{k}_c}^{(1)} | i \hbar \partial_t | \Psi_{\mathbf{x}_c, \mathbf{k}_c}^{(1)} \rangle \\ &= \frac{1}{2} \sum_{l(\neq n)} \left( M_{ln, \mathbf{k}_c}^{(1)*} (i \hbar \partial_t M_{ln, \mathbf{k}_c}^{(1)}) - (i \hbar \partial_t M_{ln, \mathbf{k}_c}^{(1)*}) M_{ln, \mathbf{k}_c}^{(1)} \right) \\ &- i \hbar \partial_t \delta - 2\hbar \delta \partial_t \gamma_{n\mathbf{k}_c}. \end{aligned} \quad (\text{C9})$$

Hence the dynamical energy can be summarized by accompanying Eqs.(C8) and (C9) as,

$$\mathcal{E}_n^{\text{dyn}(2)} = -\frac{1}{2} \sum_{l(\neq n)} \left( M_{ln, \mathbf{k}_c}^{(1)*} (i \hbar \partial_t M_{ln, \mathbf{k}_c}^{(1)}) - (i \hbar \partial_t M_{ln, \mathbf{k}_c}^{(1)*}) M_{ln, \mathbf{k}_c}^{(1)} \right). \quad (\text{C10})$$

If the Hamiltonian carries no  $\mathbf{x}_c$ -dependence and the magnetization precesses around one axis, then the explicit form of the perturbation coefficient  $M_{ln, \mathbf{k}_c}^{(1)}$  is known. Substituting it into Eqs.(C6) and (C10), the energy of the wave-packet can be summarized as follows.

$$\begin{aligned}
\mathcal{E}_n^{(2)} &= \sum_{l(\neq n)} \varepsilon_{ln}^{(0)}(\mathbf{x}_c, \mathbf{m}_0) M_{ln, \mathbf{k}_c}^{(1)*} M_{ln, \mathbf{k}_c}^{(1)} + \sum_{\beta} 2\text{Re} \left[ \sum_{l(\neq n)} M_{ln, \mathbf{k}_c}^{(1)} (\hat{H}'_{\beta})_{ln} \right] \delta m_{\beta}(t) - \frac{1}{2} \sum_{l(\neq n)} \left( M_{ln, \mathbf{k}}^{(1)*} (i\hbar \partial_t M_{ln, \mathbf{k}}^{(1)}) - (i\hbar \partial_t M_{ln, \mathbf{k}}^{(1)*}) M_{ln, \mathbf{k}}^{(1)} \right) \\
&= J_{\text{ex}}^2 \sum_{\alpha, \beta} \text{Re} \left[ \sum_{l(\neq n)} \frac{\varepsilon_{nl}^{(0)}(\mathbf{x}_c, \mathbf{m}_0) \sigma_{\alpha}^{nl} \sigma_{\beta}^{ln}}{(\varepsilon_{nl}^{(0)}(\mathbf{x}_c, \mathbf{m}_0))^2 - \hbar^2 \omega^2} \right] \delta m_{\alpha}(t) \delta m_{\beta}(t) + J_{\text{ex}}^2 \sum_{\alpha, \beta} \text{Im} \left[ \sum_{l(\neq n)} \frac{\sigma_{\alpha}^{nl} \sigma_{\beta}^{ln}}{(\varepsilon_{nl}^{(0)}(\mathbf{x}_c, \mathbf{m}_0))^2 - \hbar^2 \omega^2} \right] \delta m_{\alpha}(t) \delta \dot{m}_{\beta}(t).
\end{aligned} \tag{C11}$$

#### Appendix D: Definition of normalized quantum geometric tensor

Since the normalized quantum geometric quantities are used both in the main text and in this Appendix, we summarize them here. To this end, we consider the situation as the same as Sec. III in the main text, where  $\mathbf{x}_c$ -dependence no longer exists. The conventional Quantum geometric tensor is defined as  $\mathcal{Q}_{\mu\nu}^{\xi\xi', nl} = \mathcal{A}_{\mu}^{\xi, nl} \mathcal{A}_{\nu}^{\xi', ln}$ , where  $\mathcal{A}_{\mu}^{\xi, nl} = -i \langle u_{n\mathbf{k}}^{(0)}(\mathbf{m}_0) | \partial_{\xi_{\mu}} | u_{n\mathbf{k}}^{(0)}(\mathbf{m}_0) \rangle$ . On the other hand, the ‘‘normalized’’ quantum geometric tensor is defined as

$$\bar{\mathcal{Q}}_{\mu\nu}^{\xi\xi', nl} = \frac{(\varepsilon_{nl, \mathbf{k}}^{(0)}(\mathbf{m}_0))^2}{(\varepsilon_{nl, \mathbf{k}}^{(0)}(\mathbf{m}_0))^2 - \hbar^2 \omega^2} \mathcal{A}_{\mu}^{\xi, nl} \mathcal{A}_{\nu}^{\xi', ln}. \tag{D1}$$

As same as the conventional quantum geometric tensor, the real (imaginary) part of  $\bar{\mathcal{Q}}_{\mu\nu}^{\xi\xi', nl}$  corresponds to the quantum metric (Berry curvature),

$$\begin{aligned}
\bar{g}_{n, \mu\nu}^{\xi\xi'} &= \text{Re} \left[ \sum_{l(\neq n)} \bar{\mathcal{Q}}_{\mu\nu}^{\xi, nl} \right] \\
&= \text{Re} \left[ \sum_{l(\neq n)} \frac{(\varepsilon_{nl, \mathbf{k}}^{(0)}(\mathbf{m}_0))^2 \mathcal{A}_{\mu}^{\xi, nl} \mathcal{A}_{\nu}^{\xi', ln}}{(\varepsilon_{nl, \mathbf{k}}^{(0)}(\mathbf{m}_0))^2 - \hbar^2 \omega^2} \right], \tag{D2}
\end{aligned}$$

$$\begin{aligned}
\bar{\Omega}_{n, \mu\nu}^{\xi\xi'} &= -2\text{Im} \left[ \sum_{l(\neq n)} \bar{\mathcal{Q}}_{\mu\nu}^{\xi\xi', nl} \right] \\
&= -2\text{Im} \left[ \sum_{l(\neq n)} \frac{(\varepsilon_{nl, \mathbf{k}}^{(0)}(\mathbf{m}_0))^2 \mathcal{A}_{\mu}^{\xi, nl} \mathcal{A}_{\nu}^{\xi', ln}}{(\varepsilon_{nl, \mathbf{k}}^{(0)}(\mathbf{m}_0))^2 - \hbar^2 \omega^2} \right]. \tag{D3}
\end{aligned}$$

The Berry connection polarizability is defined as

$$\bar{G}_{n, \mu\nu}^{\xi\xi'} = \text{Re} \left[ \sum_{l(\neq n)} \frac{\varepsilon_{nl}^{(0)}(\mathbf{m}_0) \mathcal{A}_{\mu}^{\xi, nl} \mathcal{A}_{\nu}^{\xi', ln}}{(\varepsilon_{nl, \mathbf{k}}^{(0)}(\mathbf{m}_0))^2 - \hbar^2 \omega^2} \right]. \tag{D4}$$

#### Appendix E: Evaluation of first order correction for Berry connection

To compute the current based on Eq. (21), the first-order correction in the perturbation to  $\bar{\Omega}_{n, i\alpha}^{km}$  is required. As defined in Eq. (17),  $\bar{\Omega}_{n, i\alpha}^{km}$  is constructed from the Berry connection including the perturbation. We introduce the first-order correction to the Berry curvature as follows.

$$\Omega_{n, i\alpha}^{km(1)} = \partial_{k_i} A_{n, \alpha}^{m(1)} - \partial_{m_{\alpha}} A_{n, i}^{k(1)}, \tag{E1}$$

where the first-order correction to the Berry connection for  $\xi = \mathbf{k}$  or  $\mathbf{m}$  is introduced as follow,

$$\begin{aligned}
\tilde{A}_{n, \mu}^{\xi} &= -i \langle \tilde{u}_{n\mathbf{k}}(\mathbf{m}) | \partial_{\xi_{\mu}} | \tilde{u}_{n\mathbf{k}}(\mathbf{m}) \rangle \\
&= -i \langle u_{n\mathbf{k}}^{(0)}(\mathbf{m}_0) | \partial_{\xi_{\mu}} | u_{n\mathbf{k}}^{(0)}(\mathbf{m}_0) \rangle - i \langle u_{n\mathbf{k}}^{(0)}(\mathbf{m}_0) | \partial_{\xi_{\mu}} | u_{n\mathbf{k}}^{(1)}(\mathbf{m}) \rangle \\
&\quad - i \langle u_{n\mathbf{k}}^{(1)}(\mathbf{m}) | \partial_{\xi_{\mu}} | u_{n\mathbf{k}}^{(0)}(\mathbf{m}_0) \rangle + \mathcal{O}(\delta m^2) \\
&\cong A_{\mu}^{\xi(0)} + A_{\mu}^{\xi(1)}, \tag{E2}
\end{aligned}$$

$$\begin{aligned}
A_{n, \mu}^{\xi(1)} &= -i \langle u_{n\mathbf{k}}^{(0)}(\mathbf{m}_0) | \partial_{\xi_{\mu}} | u_{n\mathbf{k}}^{(1)}(\mathbf{m}) \rangle - i \langle u_{n\mathbf{k}}^{(1)}(\mathbf{m}) | \partial_{\xi_{\mu}} | u_{n\mathbf{k}}^{(0)}(\mathbf{m}_0) \rangle \\
&= 2\text{Re} \left[ -i \langle u_{n\mathbf{k}}^{(1)}(\mathbf{m}) | \partial_{\xi_{\mu}} | u_{n\mathbf{k}}^{(0)}(\mathbf{m}_0) \rangle \right]. \tag{E3}
\end{aligned}$$

In Eq. (26), we first derive the first-order correction to the  $\mathbf{m}$ -space Berry connection. By making use of Eq. (9), the calculation proceeds as follows

$$\begin{aligned}
A_{n, \alpha}^{m(1)} &= \sum_{\beta} 2\text{Re} \left[ \sum_{l(\neq n)} \frac{-i J_{\text{ex}}^2 \sigma_{\alpha}^{nl} \sigma_{\beta}^{ln}}{(\varepsilon_{nl, \mathbf{k}}^{(0)}(\mathbf{m}_0))^2 - \hbar^2 \omega^2} \left( \delta m_{\beta}(t) - i\hbar \frac{\delta \dot{m}_{\beta}(t)}{\varepsilon_{nl, \mathbf{k}}^{(0)}(\mathbf{m}_0)} \right) \right] \\
&= \sum_{\beta} 2\text{Im} \left[ \sum_{l(\neq n)} \frac{(\varepsilon_{nl, \mathbf{k}}^{(0)}(\mathbf{m}_0))^2}{(\varepsilon_{nl, \mathbf{k}}^{(0)}(\mathbf{m}_0))^2 - \hbar^2 \omega^2} \mathcal{A}_{\alpha}^{m, nl} \mathcal{A}_{\beta}^{m, ln} \right] \delta m_{\beta}(t) - 2\hbar \sum_{\beta} \text{Re} \left[ \sum_{l(\neq n)} \frac{(\varepsilon_{nl, \mathbf{k}}^{(0)}(\mathbf{m}_0))^2}{(\varepsilon_{nl, \mathbf{k}}^{(0)}(\mathbf{m}_0))^2 - \hbar^2 \omega^2} \frac{\mathcal{A}_{\alpha}^{m, nl} \mathcal{A}_{\beta}^{m, ln}}{\varepsilon_{nl, \mathbf{k}}^{(0)}(\mathbf{m}_0)} \right] \delta \dot{m}_{\beta}(t) \\
&= - \sum_{\beta} \bar{\Omega}_{n, \alpha\beta}^{mm} \delta m_{\beta}(t) - 2\hbar \sum_{\beta} \bar{G}_{n, \alpha\beta}^{mm} \delta \dot{m}_{\beta}(t)
\end{aligned} \tag{E4}$$

Here, the relation

$$\sigma_\alpha^{nl} = \frac{\varepsilon_{nl,\mathbf{k}}^{(0)}(\mathbf{m}_0)}{J_{\text{ex}}} i \mathcal{A}_\alpha^{m,nl} \quad (\text{E5})$$

where  $\mathcal{A}_\alpha^{m,nl} = -i \langle u_{n\mathbf{k}}^{(0)}(\mathbf{m}_0) | \partial_{m_\alpha} | u_{l\mathbf{k}}^{(0)}(\mathbf{m}_0) \rangle$  has been employed to derive the second line of Eq. (E4). For the  $\mathbf{k}$ -

space Berry connection, we calculate its first-order correction for the perturbation as well as the  $\mathbf{m}$ -space one. Using the relation

$$v_i^{nl} = -\varepsilon_{nl,\mathbf{k}}^{(0)}(\mathbf{m}_0) i \mathcal{A}_i^{k,nl} \quad (\text{E6})$$

where  $\mathcal{A}_i^{k,nl} = -i \langle u_{n\mathbf{k}}^{(0)}(\mathbf{m}_0) | \partial_{k_i} | u_{l\mathbf{k}}^{(0)}(\mathbf{m}_0) \rangle$ , we get the following result,

$$\begin{aligned} A_{n,j}^{k(1)} &= \sum_\beta 2\text{Im} \left[ \sum_{l(\neq n)} \frac{(\varepsilon_{nl,\mathbf{k}}^{(0)}(\mathbf{m}_0))^2}{(\varepsilon_{nl,\mathbf{k}}^{(0)}(\mathbf{m}_0))^2 - \hbar^2 \omega^2} \mathcal{A}_j^{k,nl} \mathcal{A}_\beta^{m,ln} \right] \delta m_\beta(t) - 2 \sum_\beta \text{Re} \left[ \sum_{l(\neq n)} \frac{(\varepsilon_{nl,\mathbf{k}}^{(0)}(\mathbf{m}_0))^2}{(\varepsilon_{nl,\mathbf{k}}^{(0)}(\mathbf{m}_0))^2 - \hbar^2 \omega^2} \frac{\mathcal{A}_j^{k,nl} \mathcal{A}_\beta^{m,ln}}{\varepsilon_{nl,\mathbf{k}}^{(0)}(\mathbf{m}_0)} \right] \delta \dot{m}_\beta(t), \\ &= - \sum_\beta \bar{\Omega}_{n,j\beta}^{km} \delta m_\beta(t) - 2 \sum_\beta \bar{G}_{n,j\beta}^{km} \delta \dot{m}_\beta(t). \end{aligned} \quad (\text{E7})$$

## Appendix F: Formulae of precession current for numerical calculations

Derivatives of the quantum geometric quantities appear in the expressions for the nonlinear current. In the numerical calculations presented in Sec.IV B, these derivatives are rewritten in terms of matrix elements of the velocity or spin operators. By using Eqs.(E5) and (E6), and the relation of the complete system with respect to  $|u_{n\mathbf{k}}^{(0)}(\mathbf{m}_0)\rangle$ , we get the following formulae,

$$\begin{aligned} \partial_{m_\alpha} v_i^{nl} &= \langle \partial_{m_\alpha} u_{n\mathbf{k}}^{(0)}(\mathbf{m}_0) | \hat{v}_i | u_{l\mathbf{k}}^{(0)}(\mathbf{m}_0) \rangle + \langle u_{n\mathbf{k}}^{(0)}(\mathbf{m}_0) | \hat{v}_i | \partial_{m_\alpha} u_{l\mathbf{k}}^{(0)}(\mathbf{m}_0) \rangle \\ &= \sum_m \langle \partial_{m_\alpha} u_{n\mathbf{k}}^{(0)}(\mathbf{m}_0) | u_{m\mathbf{k}}^{(0)}(\mathbf{m}_0) \rangle \langle u_{m\mathbf{k}}^{(0)}(\mathbf{m}_0) | \hat{v}_i | u_{l\mathbf{k}}^{(0)}(\mathbf{m}_0) \rangle + \sum_m \langle u_{n\mathbf{k}}^{(0)}(\mathbf{m}_0) | \hat{v}_i | u_{m\mathbf{k}}^{(0)}(\mathbf{m}_0) \rangle \langle u_{m\mathbf{k}}^{(0)}(\mathbf{m}_0) | \partial_{m_\alpha} u_{l\mathbf{k}}^{(0)}(\mathbf{m}_0) \rangle \\ &= -J_{\text{ex}} \sum_{m(\neq n)} \frac{\sigma_\alpha^{nm} v_i^{ml}}{\varepsilon_{nm,\mathbf{k}}^{(0)}(\mathbf{m}_0)} + J_{\text{ex}} \sum_{m(\neq l)} \frac{v_i^{nm} \sigma_\alpha^{ml}}{\varepsilon_{ml,\mathbf{k}}^{(0)}(\mathbf{m}_0)} \end{aligned} \quad (\text{F1})$$

$$\begin{aligned} \partial_{k_i} \sigma_\alpha^{nl} &= \langle \partial_{k_i} u_{n\mathbf{k}}^{(0)}(\mathbf{m}_0) | \hat{\sigma}_\alpha | u_{l\mathbf{k}}^{(0)}(\mathbf{m}_0) \rangle + \langle u_{n\mathbf{k}}^{(0)}(\mathbf{m}_0) | \hat{\sigma}_\alpha | \partial_{k_i} u_{l\mathbf{k}}^{(0)}(\mathbf{m}_0) \rangle \\ &= \sum_m \langle \partial_{k_i} u_{n\mathbf{k}}^{(0)}(\mathbf{m}_0) | u_{m\mathbf{k}}^{(0)}(\mathbf{m}_0) \rangle \langle u_{m\mathbf{k}}^{(0)}(\mathbf{m}_0) | \hat{\sigma}_\alpha | u_{l\mathbf{k}}^{(0)}(\mathbf{m}_0) \rangle + \sum_m \langle u_{n\mathbf{k}}^{(0)}(\mathbf{m}_0) | \hat{\sigma}_\alpha | u_{m\mathbf{k}}^{(0)}(\mathbf{m}_0) \rangle \langle u_{m\mathbf{k}}^{(0)}(\mathbf{m}_0) | \partial_{k_i} u_{l\mathbf{k}}^{(0)}(\mathbf{m}_0) \rangle \\ &= \sum_{m(\neq n)} \frac{v_i^{nm} \sigma_\alpha^{ml}}{\varepsilon_{nm,\mathbf{k}}^{(0)}(\mathbf{m}_0)} - \sum_{m(\neq l)} \frac{\sigma_\alpha^{nm} v_i^{ml}}{\varepsilon_{ml,\mathbf{k}}^{(0)}(\mathbf{m}_0)} \end{aligned} \quad (\text{F2})$$

$$\begin{aligned} \partial_{m_\alpha} \sigma_\beta^{ln} &= \langle \partial_{m_\alpha} u_{l\mathbf{k}}^{(0)}(\mathbf{m}_0) | \hat{\sigma}_\beta | u_{n\mathbf{k}}^{(0)}(\mathbf{m}_0) \rangle + \langle u_{l\mathbf{k}}^{(0)}(\mathbf{m}_0) | \hat{\sigma}_\beta | \partial_{m_\alpha} u_{n\mathbf{k}}^{(0)}(\mathbf{m}_0) \rangle \\ &= \sum_m \langle \partial_{m_\alpha} u_{l\mathbf{k}}^{(0)}(\mathbf{m}_0) | u_{m\mathbf{k}}^{(0)}(\mathbf{m}_0) \rangle \langle u_{m\mathbf{k}}^{(0)}(\mathbf{m}_0) | \hat{\sigma}_\beta | u_{n\mathbf{k}}^{(0)}(\mathbf{m}_0) \rangle + \sum_m \langle u_{l\mathbf{k}}^{(0)}(\mathbf{m}_0) | \hat{\sigma}_\beta | u_{m\mathbf{k}}^{(0)}(\mathbf{m}_0) \rangle \langle u_{m\mathbf{k}}^{(0)}(\mathbf{m}_0) | \partial_{m_\alpha} u_{n\mathbf{k}}^{(0)}(\mathbf{m}_0) \rangle \\ &= J_{\text{ex}} \sum_{m(\neq l)} \frac{\sigma_\alpha^{lm} \sigma_\beta^{mn}}{\varepsilon_{ml,\mathbf{k}}^{(0)}(\mathbf{m}_0)} - J_{\text{ex}} \sum_{m(\neq n)} \frac{\sigma_\beta^{lm} \sigma_\alpha^{mn}}{\varepsilon_{nm,\mathbf{k}}^{(0)}(\mathbf{m}_0)} \end{aligned} \quad (\text{F3})$$

Employing the above formulae, for instance, the derivative of the normalized Berry curvature  $\Omega_{n,i\beta}^{km}$  can read as

$$\begin{aligned}
\partial_{m_\alpha} \overline{\Omega}_{n,i\beta}^{km} &= 2J_{\text{ex}} \text{Im} \left[ \sum_{l(\neq n)} \partial_{m_\alpha} \left( \frac{v_i^{nl} \sigma_\beta^{ln}}{(\varepsilon_{nl,\mathbf{k}}^{(0)}(\mathbf{m}_0))^2 - \hbar^2 \omega^2} \right) \right] \\
&= -2J_{\text{ex}}^2 \sum_{l(\neq n)} \text{Im} \left[ -2 \frac{\varepsilon_{nl,\mathbf{k}}^{(0)}(\mathbf{m}_0) (\sigma_\alpha^{nn} - \sigma_\alpha^{ll})}{((\varepsilon_{nl,\mathbf{k}}^{(0)}(\mathbf{m}_0))^2 - \hbar^2 \omega^2)^2} v_i^{nl} \sigma_\beta^{ln} \right. \\
&\quad \left. + \sum_{m(\neq n)} \frac{\sigma_\alpha^{nm} v_i^{ml} \sigma_\beta^{ln} + v_i^{nl} \sigma_\beta^{lm} \sigma_\alpha^{mn}}{\varepsilon_{nm,\mathbf{k}}^{(0)}(\mathbf{m}_0) ((\varepsilon_{nl,\mathbf{k}}^{(0)}(\mathbf{m}_0))^2 - \hbar^2 \omega^2)} - \sum_{m(\neq l)} \frac{v_i^{nm} \sigma_\alpha^{ml} \sigma_\beta^{ln} + v_i^{nl} \sigma_\alpha^{lm} \sigma_\beta^{mn}}{\varepsilon_{ml,\mathbf{k}}^{(0)}(\mathbf{m}_0) ((\varepsilon_{nl,\mathbf{k}}^{(0)}(\mathbf{m}_0))^2 - \hbar^2 \omega^2)} \right], \quad (\text{F4})
\end{aligned}$$

and other derivative can be obtained as same as the above calculation.

---